



University of Kentucky
UKnowledge

KWRRRI Research Reports

Kentucky Water Resources Research Institute

5-2-1974

Laboratory Simulation of Rainfall Erosivity for Gully Formation Study

Digital Object Identifier: <https://doi.org/10.13023/kwrrri.rr.73>

T. Y. Kao
University of Kentucky

Right click to open a feedback form in a new tab to let us know how this document benefits you.

Follow this and additional works at: https://uknowledge.uky.edu/kwrrri_reports

 Part of the [Atmospheric Sciences Commons](#), [Meteorology Commons](#), and the [Soil Science Commons](#)

Repository Citation

Kao, T. Y., "Laboratory Simulation of Rainfall Erosivity for Gully Formation Study" (1974). *KWRRRI Research Reports*. 123.
https://uknowledge.uky.edu/kwrrri_reports/123

This Report is brought to you for free and open access by the Kentucky Water Resources Research Institute at UKnowledge. It has been accepted for inclusion in KWRRRI Research Reports by an authorized administrator of UKnowledge. For more information, please contact UKnowledge@lsv.uky.edu.

LABORATORY SIMULATION OF
RAINFALL EROSIVITY FOR
GULLY FORMATION STUDY

By

T. Y. Kao
Principal Investigator

Project Number A-037-KY (Partial Completion Report)
Agreement Numbers: 14-31-0001-3517 (FY 1971)
14-31-0001-3817 (FY 1972)
Period of Project: August, 1971 - June, 1973

University of Kentucky Water Resources Institute
Lexington, Kentucky

The work upon which this report is based was supported in part by funds provided by the United States Department of the Interior, Office of Water Resources Research, as authorized under the Water Resources Research Act of 1964

May 2, 1974

ABSTRACT

The objective of this study was to develop a rainfall simulator, which imparts to the laboratory rainfall the more important characteristics of natural rainfall such as intensity, drop spectrum, kinetic energy, and momentum at impact, for using in soil erosion research with better results. In developing this simulator the better features of the basic types of earlier simulators, drip and nozzle, have been incorporated into this single desing. The simulator developed in this study consists of a number of individual box modules placed in a rectangular pattern to form a single unit. Each module has a grid of capillary holes with cone shaped exits drilled through the bottom plate. The modules were mounted so that their bottom plates form the ceiling of a pressurized room. This provides a hydrostatic pressure differential between the bottom plate and the water surface in each module, such that water will not leak through the holes during the nonoperating state. When pressure pulses are applied to the water surface in each module, water drops are ejected with an initial velocity so that a terminal velocity corresponding to a natural rain drop can be attained without requiring excessive height of fall. The test results indicated that this simulator provides good simulation of the natural rainfall erosivity.

KEY WORDS: rainfall simulation, soil erosion, water drops, kinetic energy, momentum, erosivity index.

TABLE OF CONTENTS

	Page
ACKNOWLEDGMENTS	iii
LIST OF FIGURES	v
LIST OF TABLES.	vii
 CHAPTER	
I INTRODUCTION.	1
Review of Previous Work	2
a. Drip Simulators	3
b. Nozzle Simulators	5
Pulse Pressure Rainfall Module.	10
II THE DEVELOPMENT OF THE NEW RAINFALL SIMULATOR	12
Rainfall Module	13
Static Pressure Room.	17
Rainfall Simulator Arrangement.	19
Water Supply System	21
Air Supply and Pulse Control.	21
III EXPERIMENTAL PROCEDURES	32
Determination of Water Drop Velocity.	32
Measurement of Simulated Raindrop Size.	36
Simulated Rainfall Intensity.	36
IV ANALYSIS OF RESULTS	39
Derivation of Velocity-Fall Distance Relationships	39
Rainfall Simulator Characteristics.	45
Relative Erosivity Ratio.	50
V SUMMARY AND CONCLUSIONS	56
REFERENCES.	59
NOTATION.	

LIST OF FIGURES

Figure		Page
1	Rainfall Module	15
2	Rainfall Module Construction.	16
3	Schematics of the Rainfall Module Installation and Pressurized Room for Water Head, h, Retention.	18
4	Mounting Frame for Modules.	20
5	Installation of Rainfall Modules.	20
6	Water Supply System	22
7	Water Supply and Siphon Tubes	23
8	Constant Head Tank.	23
9	Schematics of the Pressure Pulse Supply System	25
10	Air Distribution System	26
11	Rotating Valve for Pressure Pulse Distribution.	27
12	Rotating Valve Assembly and Speed Control	29
13A	Drop Velocity Measuring Arrangement	34
13	Pressure Pulse Distribution Valve	26
14	Experimental Setup for Velocity Determination	35
15	Multiple Image Stroboscopic Photograph for Drop Size and Velocity Measurement.	35
16	Drop Stain on Whatman No. 1 Filter Paper.	37
17	Definition Sketch of Water Drop Falling Through a Resistive Medium.	39
18	Relationship Between Rain Drop Diameter and Fall Velocity	43
19	Rainfall Simulator Operation Characteristics.	48

LIST OF FIGURES (Cont.)

Figure		Page
20	Rainfall Intensity and Drop Diameter Relationship.	49
21	Relative Erosivity Ratio of the Simulated Rainfall at Eight Feet of Fall.	51
22	Relative Erosivity Ratio of the Simulated Rainfall at Ten Feet of Fall.	52
23	Relative Erosivity Ratio of the Simulated Rainfall at Twelve Feet of Fall	53

LIST OF TABLES

Table		Page
I	Drop Velocity Computation	44
II	Relative Erosivity Computation.	46
III	Simulated Rainfall Data	47
IV	Relative Erosivity Ratio.	54

CHAPTER I
INTRODUCTION

For many years, rainfall simulators have been used to accelerate research in areas concerning soil erosion mechanics and surface runoff hydrology by research workers in various disciplines. The basic requirement in developing a prototype simulator includes being able to control rainfall intensity, drop spectrum, and provide drop velocities near that of natural rainfall. A rainfall simulator has many advantages as a research tool. Among these advantages are: tests can be conducted at any time without delay, experiments can be carried out efficiently, and close control can be exercised over the intensity and duration of the simulated rainfall.

In general rainfall simulators can be divided into two types, drip simulators and nozzle simulators. The former utilizes the capillary effect to produce drops of required size at zero initial velocity. Because the velocity of the drop is attained by free fall to a test plot, excessive heights of fall are required in order for the impact velocity to approach that of natural rain. This limits the use of this type simulator in studies of the mechanics of soil erosion.

A nozzle simulator produces a drop distribution that includes a large range of drop sizes with nonzero initial velocity. However, when a large rainfall intensity is required, while facilitating the attainment of higher impact velocities, the increased operating pressure causes the drop size to be reduced. The drops in some instances become a mist. If high discharge nozzles are used to provide suitable drop sizes while maintaining desired velocities, very high application rates often result.

The deficiencies in these simulators lead to the development of a new type simulator which utilizes in part capillary force and pressure differential to hold the water head in the rainfall module, surface tension to form drops and, in particular, the periodic pressure pulse to eject the water drop at a desirable initial velocity. A detailed design feature of such a new rainfall simulator developed in this study and its calibration procedure and results are described and presented in latter sections as part of this report.

Review of Previous Work

Over the years, there have been several simulators built such as those at Purdue University, University of Illinois, Iowa State University, Massachusetts Institute of Technology, and many other institutions. These simulators are of either drip or nozzle types. A brief summary of these instruments is presented in the following section.

a. Drip Simulators

Among those drip simulators hanging yarn, hypodermic needles, or graded tubes have been used to produce drops of the required size at zero initial velocity. Ellison and Pomerne (1) have shown details of a simulator using hanging yarn. This type drop former was also mentioned earlier by Parsons (2) and referred to as a "dripulator" or "stalactometer" rainfall simulator. The main part of this simulator consists of a muslin or cheese cloth laid loosely over a chicken wire screen such that a depression in the cloth forms at each opening in the screen. A piece of yarn was then attached to the cloth at each depression. Thus, water applied as a spray to the cloth collected at the depression and traveled down the hanging yarn to form drops. The average intensity was easily controlled either by flow through the supply nozzle, or by the head in a supply tank mounted above the drop forming system. The drop size was dependent on the yarn size and was limited to a diameter larger than 4 mm (0.157 in).

The use of tube tips as a drop former is a more precise method of producing waterdrops. Ekern and Muckenhirn (3) used a simulator made of 22 gage hypodermic needles set in a 10 quart aluminum container on a one inch grid. The needles were enclosed in various sizes of glass tubing to change drop sizes from 2.8 to 5.8 mm (0.110 to 0.228 in). The drops approached terminal velocity by

by virtue of a 10.67 m (35 ft) fall. It was also noted that in this height of fall that air currents deflected the drops thus producing a random impact pattern at the plot surface.

A simulator using a telescoping of tubes was developed by Mutchler and Moldendauer (4). While smaller tubes at the top control the flowrate, larger tubes at the bottom form the desired drop size. The intensity was controlled by size selection of the smallest tube in the drop former, the density of drop formers in the applicator and the head of water above the drop former. The drop formers were set in a donut-shaped applicator tank which rotated to give a uniform intensity distribution. Palmer (5) also developed a simulator which used a series of graded stainless steel tubes to control the flow rate and produce the desired drop size. The height of fall from the applicator to the test plot was adjustable so that the energy at impact could be varied.

Similarly, Grace and Eagleson (6) used stainless steel needles. The needles were placed in the bottom of one foot square resin boxes. A line connecting a head tank to this box permitted this simulator to generate intensities from 12.7 to 1270 mm/hr (0.5 to 50 in/hr).

The principle limitation of capillary techniques is the height of fall necessary to attain at least 95% of the terminal velocity. This height of fall was considered to

vary from 5 m (16.40 ft) for a drop 2 mm (0.079 in) in diameter to 8 m (26.25 ft) for a drop 4 mm (0.157 in) in diameter. Laws (7) has shown that the terminal velocity of a raindrop is not necessarily a definite value. This is due to the fact that the shape of raindrops vary from oblate to prolate as they fall.

b. Nozzle Simulators

The second category are simulators which use nozzle drop formers to produce different initial velocities by varying the applied pressure. This made the task of generating drops near terminal velocity within a reasonable distance below the drop former an easy one. The major difficulties with nozzle simulators are that the flow rate is often too high to use in a steady application and no definite or consistent relationship can be determined between nozzle pressure, drop size and intensity.

The intensity of nozzle simulators can be evenly distributed by moving the spray pattern back and forth across the test area. This can be done by oscillating the nozzle from a fixed position or by mounting the nozzle on a reciprocating carriage. The problem of high flow rates of many nozzles can be solved by moving the spray off the test area in effect provide an on and off spray. The disadvantage of this solution is that the average magnitude which is produced by high and zero intensity periods is used to represent the continuous natural rainfall intensity.

Some of the earlier nozzle systems were ordinary sprinkling cans. The system used by Lowdermilk (8) consisted of two horizontal pipes fitted with orifices and placed on each side of the test plot. Craddock and Pearse (9) used 0.79 mm (0.031 in) orifice nozzles. The intensity distribution of their system was obtained by oscillating the delivery pipes and nozzles to move the spray back and forth across the test plot. More studies during the 1930's were made by Duley and Hays (10) and Nichols and Sexton (11). At the time of those studies, the lack of quantitative information made it impossible to produce rainfall that was representative of natural rainfall. It was also noted that the importance of the impact of raindrops was not generally recognized when these studies were made.

Major advances in nozzle design began with the interest given to simulated rainfall by Soil Conservation Service workers in the National Bureau of Standards as described by Parsons (2). Through their work the type D, E, and F apparatus were developed.

With the nozzle spraying downward, the type D apparatus was developed using modified Grinnell 1.5 nozzles. On the other hand the type E apparatus used the modified Skinner-Catfish nozzle to produce upward spray. The distribution for this apparatus was dependent upon the spray pattern and the spacing. After the disclosure by

Laws (7), that raindrop fall velocity varies with drop size and distance of fall, Young (12) developed the type F apparatus which produced a drop size distribution similar to that of high intensity rainfall. Drops from this nozzle also sprayed upward and fell an average height of 2.44 m (3.0 ft). This resulted in a velocity of fall less than the terminal velocity for most of the drops. The type F apparatus has two distinct disadvantages as does the hanging yarn method described previously. It requires wind shields for low wind velocities and an excessive height of fall for the drops to approach terminal velocity.

The most suitable nozzle for raindrop simulators has been the 80100 VeeJet commercial nozzle used by Meyer and McCune (13) in the simulator called the "Rainulator". The nozzle, at 1050 N/M^2 (6.0 lb/in^2) line pressure and spraying downward, produced a drop size distribution similar to that of natural rainfall. The median drop size, based on volume, was about 2.13 mm (0.084 in) in diameter compared with 2.50 mm (0.098 in) diameter of rainfall at an intensity of 50.80 mm/hr (2.0 in/hr). The kinetic energy developed by the nozzle at 2.44 m (8.0 ft) height as used in the "Rainulator" was about 80% of that of similar intensity rainfalls. Another simulator along the same line called the "16 Unit Rainulator" was developed by Hersmeier et al (14).

Bubbenzer and Meyer (15) developed a simulator using three 80100 VeeJet nozzles spraying downward from a height of 2.44 M (8.0 ft) onto the test plot. To obtain a high energy at a reasonable intensity, the nozzles were oscillated across the plot. The movement was similar to an eccentric drive, except there was a delay after each half cycle. Thus, periods without application are very short yet most of the nozzles spray did not reach the test plot.

The horizontal component of drop velocity was minimized by having the nozzle orifice on the centerline of the oscillating shaft. The movement of the nozzle, therefore did not impart any additional horizontal component of velocity to the spray. The drop size distribution and average fall velocities were similar to those of the "Rainulator", developed by Meyer and McCune (13).

The "Rainulator" and the "16 Unit Rainulator" were both portable, but the time required for set up was quite long. Besides, the apparatus were expensive and required a skilled crew to operate. Swanson (16) developed another simulator mounted on a trailer with a rotating-boom for distribution. Thus, decreasing set up time and requiring less skill for its operation. This simulator has certain inherent undesirable characteristics. Among these characteristics are: the cycling of simulated rainfall

varies over the plot; the nozzle heights are lower over the upper end of the plot; and water is distributed in a circular pattern requiring protection for immediate adjacent plots. However, these characteristics have neither affected the results obtained nor proven to be a problem in the use of the simulator.

Shachori and Seginer (17) used a two-arm rotating sprinkler system to simulate natural rainfall. The application of water by the system was found to be within 8% of natural rainfall application. It was also possible to simulate any desired intensity between 6 and 120 mm/hr (0.24 and 4.72 in/hr). At these intensities the measured impact velocity of the drops was used to compare with those determined by Gunn and Kinzer (18), and for small drop sizes 1 mm (0.039 in) the ratio of velocities was 0.98 and 4 mm (0.157 in) drops a ratio of 0.76.

Yet another simulator which used the nozzle as a drop former was developed by Morin, Goldberg, and Seginer (19). This simulator covered an area of 1.5 m^2 (16.14 ft^2) which is small compared to other test plots. Although, the drop spectrum was predominantly large drops, it did produce velocities near the terminal velocity of natural raindrops, by using high discharge, wide angle, full cone nozzles. The intensity was controlled by adjusting the angular speed of a rotating disk with a section aperture mounted below the downward spraying nozzle. The

comparison of the results produced in this study with those gathered by Laws (7) on natural rainfall characteristics, show close agreement. It was also indicated, that energy characteristics of natural rain are far from being a single valued function of the intensity. For intensities up to 50 mm/hr (1.97 in/hr) the simulator is able to produce a variety of energies which cover the whole range of natural rainfall characteristics for a limited application area.

Pulse Pressure Rainfall Module

In an effort to bring together the advantageous features of both drip and nozzle simulators, a unique rainfall simulator has been developed in this study. Although the drops fall only 3.05 m (10. ft) they approach terminal velocity by virtue of an initial velocity provided by a periodic pressure pulse at the beginning of fall. The simulator is also able to produce a drop spectrum in the range of natural rainfall. One of the most important features of this simulator is that the intensity and drop size can be controlled separately. Therefore uniform application rates can be achieved without sacrificing drop size or velocity. The test area under this simulator is 3.72 m^2 (40 ft^2) which can be expanded by installing additional $0.305 \text{ m} \times 0.305 \text{ m}$ (1 ft x 1 ft) rainfall modules of desired number.

It should be emphasized that the difficulties in comparing artificial rain with natural rain is due to both the lack of suitable parameters to make the comparison, and the lack of data concerning the detailed characteristics of natural rainfall. This can be seen by the fact that available data on rainfall characteristics, such as those presented by Laws (7), and Gunn and Kinzer (18) differ widely from one another. Therefore, in developing this simulator it is intended to provide a close simulation of natural rain under a controlled environment. So that the role of rain drop impact in the process of soil erosion can be closely observed, the latter part of this task will be reported separately and is not included in this report.

CHAPTER II

THE DEVELOPMENT OF THE NEW RAINFALL SIMULATOR

The simulators developed thus far have deficiencies which prevented them from producing rainfall representative of natural rain. As discussed in the previous chapter, drip simulators require the installation of graded capillary tubes for each drop, to control the flow rate and drop size. Considering thousands of drops are produced for a simulator of moderate size this process is not only laborious but very expensive.

Nozzle simulators, which utilize static pressure to control the rainfall intensity, yield no definite relationship between pressure magnitude, drop size and intensity, thus they are difficult to regulate. Although several nozzles are able to produce a drop size distribution similar to that of natural rainfall, the median drop size is low and the flow rate is often too high to use in a steady application.

Another limitation of both drip and nozzle simulators is that the initial velocity imparted to the raindrop can not be controlled. It is essential that the initial velocity be of controllable magnitude so that the raindrop

can attain its terminal velocity like natural rain within the available distance of fall. Most simulators have a limited height of fall of from 2.44 to 3.35 m (8 to 11 ft).

In order to overcome such deficiencies a new type of simulator is developed in this study to make use of several basic fluid mechanics principles. Among these, the hydrostatic pressure differential between the water surface and the bottom of the module is used to retain the water in the module. This eliminates the need for graded capillary tubes. The most important characteristic of the newly developed simulator is the use of the pressure pulse to eject the water drops at a desired initial velocity. The pressure pulses are produced by a periodic supply of compressed air to the rainfall module. By controlling the frequency and the magnitude of the pressure pulse, rain drop size and intensity may be regulated separately. This constitutes a very unique and desirable feature of this simulator.

A detailed description of the design of the simulator is given in the following sections.

Rainfall Module

The simulator system consists of forty identical individual modules. Each basic module is made of plexiglas plates to form a 0.305 m x 0.305 m (1 ft x 1 ft) box as shown in Fig. 1 and 2. The side walls of the

module are 0.64 cm (0.25 in) thick and 1.27 cm (0.50 in) and 1.90 cm (0.75 in) plates are used for top and bottom respectively. At the center of the top plate a 1.27 cm (0.50 in) I.D. brass pipe fitting is installed to connect with copper tubing for air pressure pulse supply. A 0.64 cm (0.25 in) hole drilled into a plexiglas block (A in Fig. 2) is used as the pressure release outlet to avoid any accumulative pressure build up in the module. A styrofoam ball (B in Fig. 2) attached to a 0.16 cm (0.063 in) guiding rod is resting on top of the outlet to cover the opening during the initial pulse application such that the temporary pressure increase in the module will be used to eject the water drop.

These drops are ejected through holes drilled in the 1.90 cm (0.75 in) bottom plate on 2.54 cm (1.0 in) grid. Preliminary tests indicated that 0.12 cm (0.05 in) holes provided the best results for both water retention and drop formation purposes. However, to drill thousands of such small holes to a 1.90 cm (0.75 in) depth is very difficult and almost impossible. This problem was solved by drilling 0.16 cm (0.063 in) holes and inserting in them a short section of 0.18 cm (0.07 in) O.D., 0.11 cm (0.04 in) I.D. plastic capillary tube (D in Fig. 2). The 0.32 cm (0.12 in) countersink at the bottom of each hole is designed to increase the surface area for drop formation and hold the drop in position before it is ejected.

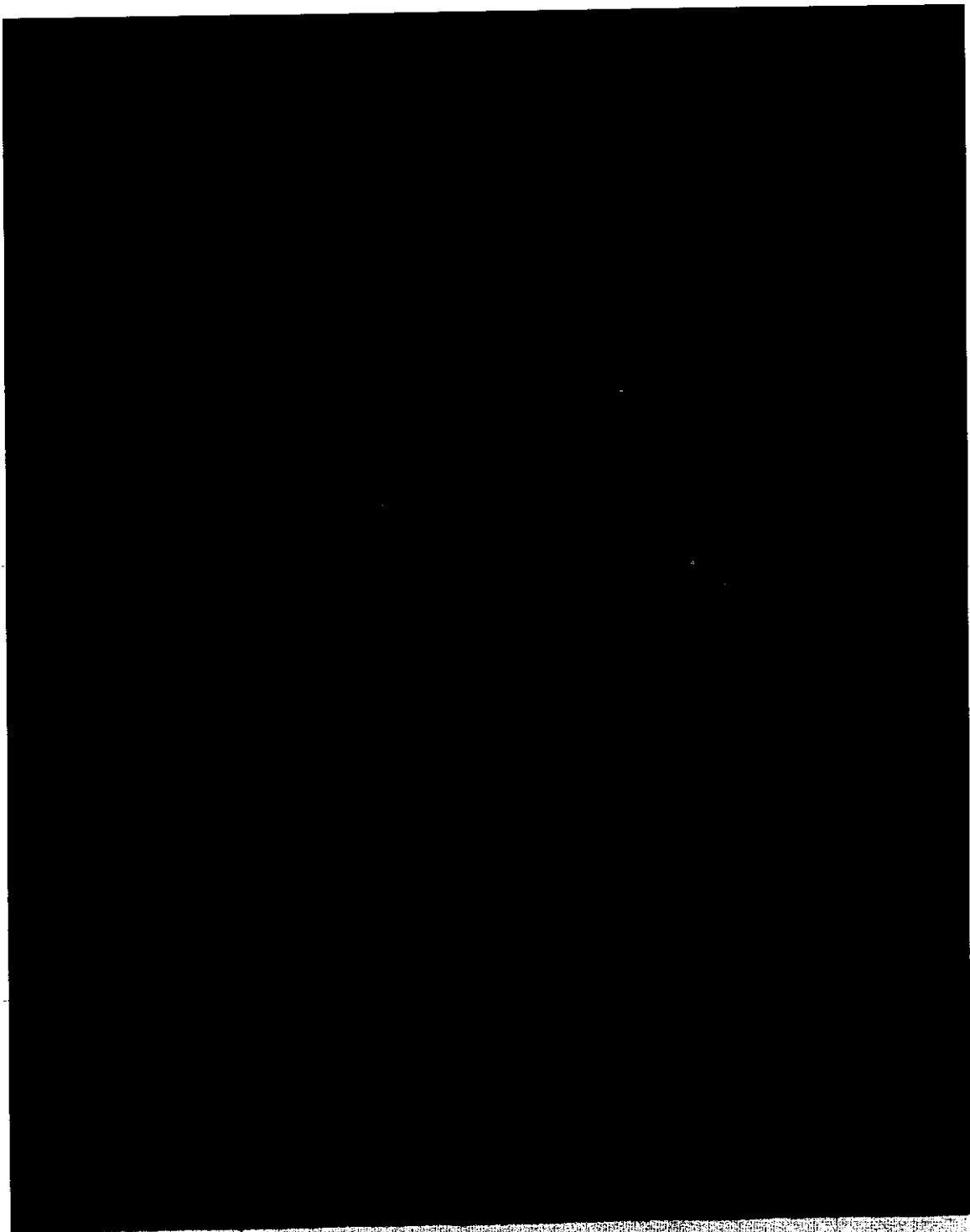


Fig. 1 Rainfall module

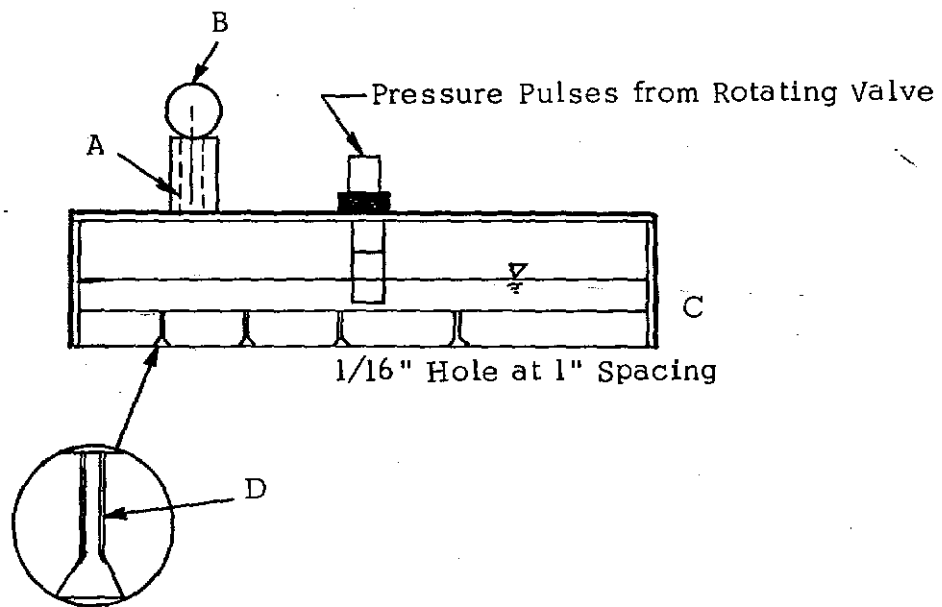
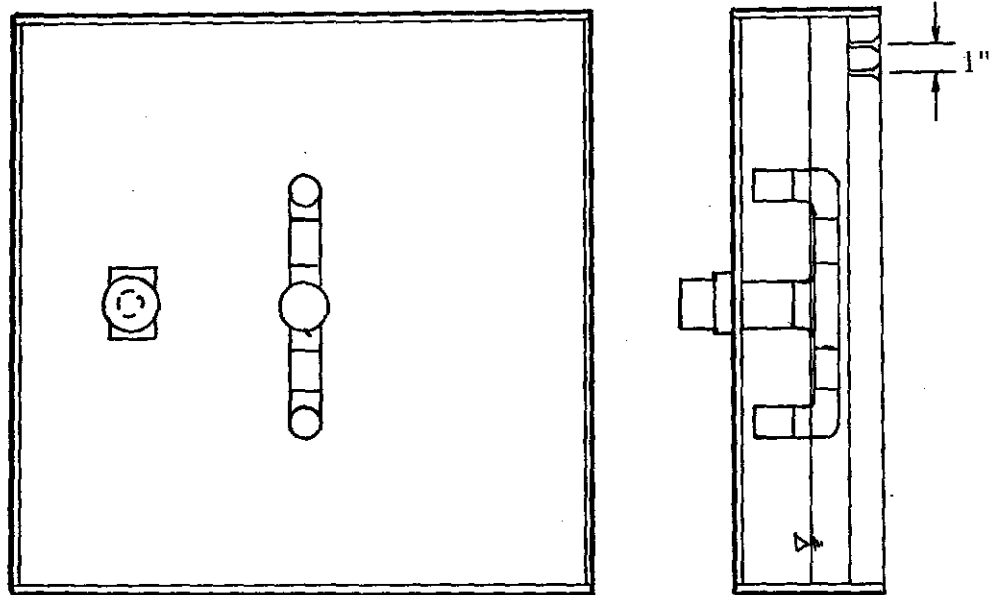


Fig.2 Rainfall Module Construction

Static Pressure Room

In the rainfall module a 3.8 cm (1.50 in) average water head measured from the lower face of the bottom plate is maintained during the time of operation. To retain this head so that water will not leak through the holes in the bottom plate a pressure differential between the water surface and the lower face of the module of the same magnitude (approximately 04.5 N/M^2 (0.54 lb/in^2) or 3.8 cm (1.50 in) water head) is required. This was accomplished by enclosing the bottom face of the module in a pressurized room, while the water surface is exposed to atmospheric pressure. This is shown schematically in Figure 3. The actual pressure room is 3.05 m (10.0 ft) wide, 4.27 m (14.0 ft) long, and 3.05 m (10.0 ft) high with the rainfall mechanism centered above it. The room is lined with polyethelene film and hardboard, sealed to the laboratory floor and to the frame which supports the rainfall simulator modules. Thus only the bottom of the rainfall modules are within the room.

Observation windows of 0.61 m (2.0 ft) width and 1.22 m (4.0 ft) length provided at eye level were installed around the room to permit observation from the outside. To avoid a sudden pressure loss while entering the room during the period of tests, a double door entrance chamber was designed. Such that before entering the inside door, the pressure within the chamber can be equilized to that

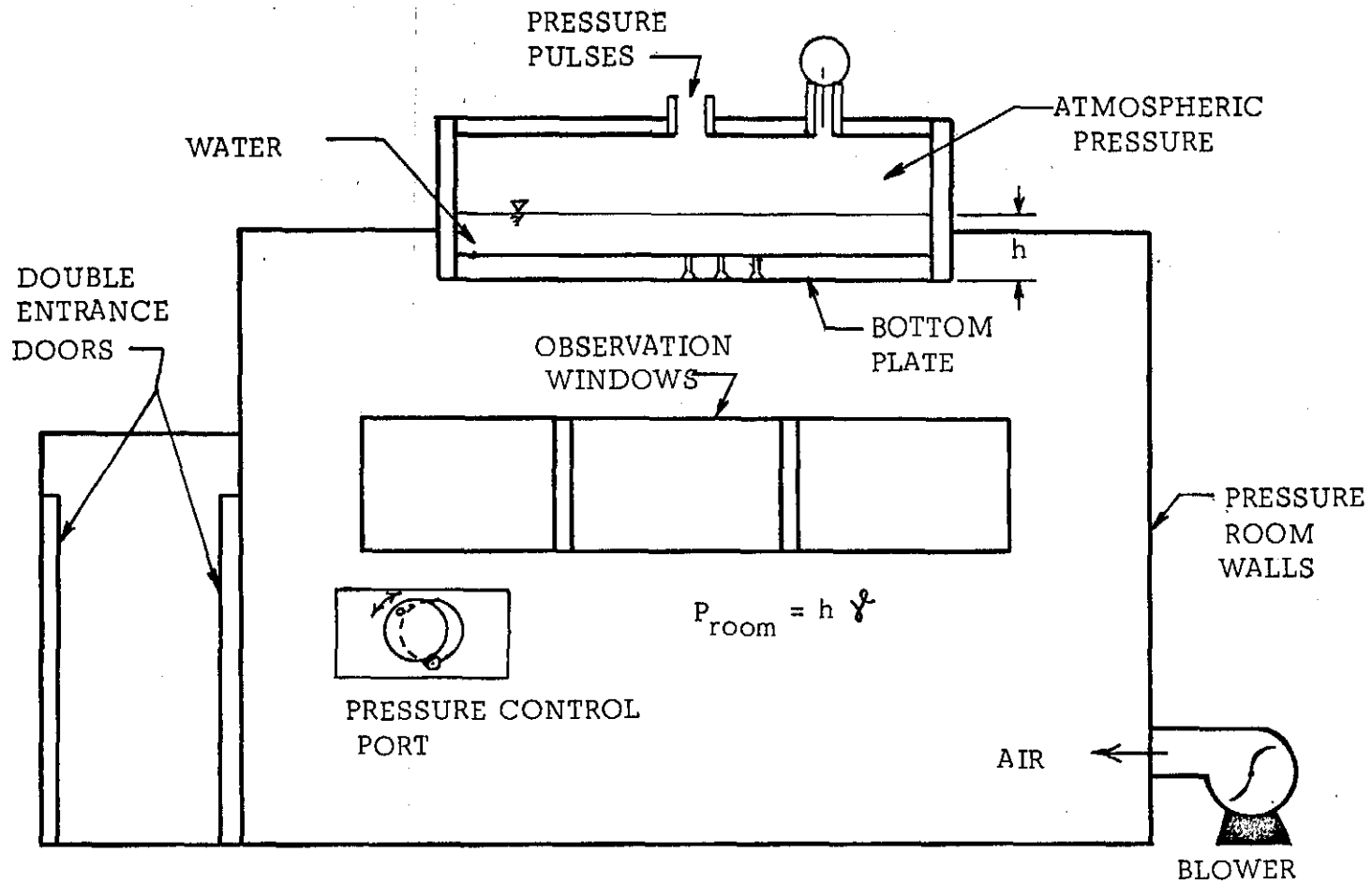


Fig. 3 Schematics of the Rainfall Module Installation and the Pressurized Room for Water Head, h , Retention

within the room by closing the outside door and letting air pressure leak slowly into the chamber.

A 11.33 m³/min (400 ft³/min) blower used to pressurize the room to approximately 9.45 N/M² (0.054 lb/in²). A 15.24 cm (6.0 in) hole through the side wall of the room with a sliding gate cover permits adjustment of the room pressure to any desired operating pressure.

Rainfall Simulator Arrangement

As described in the previous sections, the simulator is installed to form part of the ceiling of the pressure room at the center portion. The simulator which consists of 40 modules is designed to cover a 3.72 M² (40.0 ft²) test plot area. The modules are placed side by side in a 1.52 m x 2.44 m (5.0 ft x 8.0 ft) rectangular pattern. The supporting structure for the simulator are small tee rails laid across an aluminum frame as shown in Fig. 4. The 0.95 cm x 10.16 cm (0.375 in x 4.0 in) aluminum frame was bolted to 5.08 cm x 10.16 cm (2.0 in x 4.0 in) wood pieces to increase their strength and provide a place to seal the room to the mechanism. The entire frame work is supported by the end wall of the pressure room and reinforced by four 1.27 cm (0.5 in) hanging straps from the laboratory ceiling. As the boxes were placed on the tee rails they were locked together to form one unit as in Fig. 5.

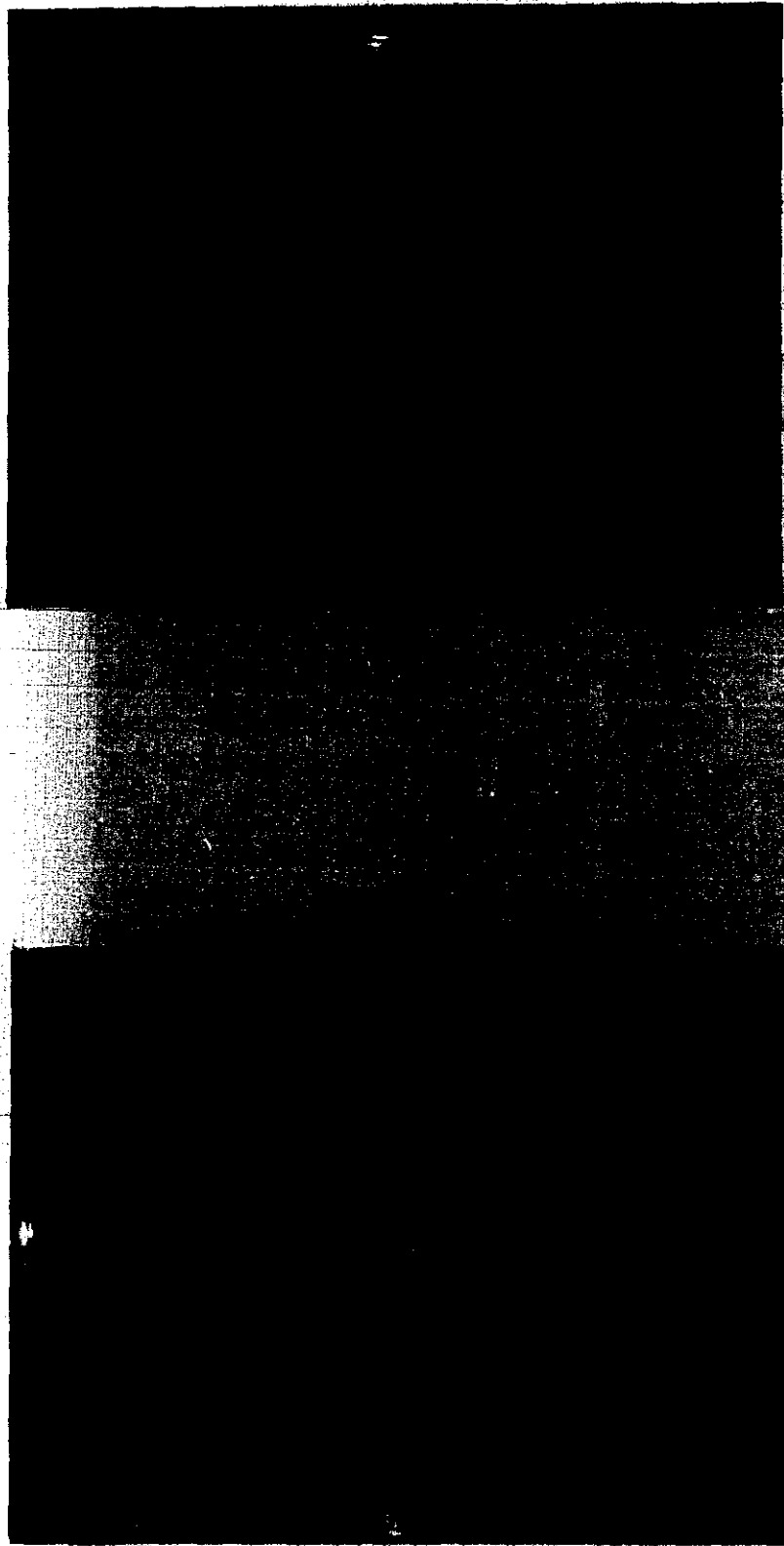


Fig. 5 Installation of rainfall modules

Water Supply System

The system used to supply water to the modules is composed of a constant head tank, four parallel water pipes, and forty siphon tubes. The 3.81 cm (1.5 in) parallel plastic pipe lines are placed on top of the simulator between every two adjacent 5 module rows Fig. 6. Ten modules are supplied by each line. At one end the four pipes are connected to a pipe the same size and in turn this line is connected to the constant head tank. On the top side of each line ten 0.64 cm (0.25 in) holes were drilled. A short section of plexiglas tube was fixed to each hole, for a tygon tubing connection. The other end of the tygon tube was connected to the rainfall modules as shown in Fig. 7 to form a siphon. A 1.90 cm (0.75 in) city water line is used to initiate flow in the system. Once the siphon is established a gradual supply can be maintained by the small head difference between the water surface in the module and the constant head tank (Fig. 8).

During the rainfall simulation, a continuous supply of water is provided through a 1.27 cm (0.5 in) water line. An adjustable overflow device within the head tank is designed to provide various head differences depending on the rainfall intensity desired.

Air Supply and Pulse Control

The method used to provide the initial velocity and eject the drop from the module is the most unique feature

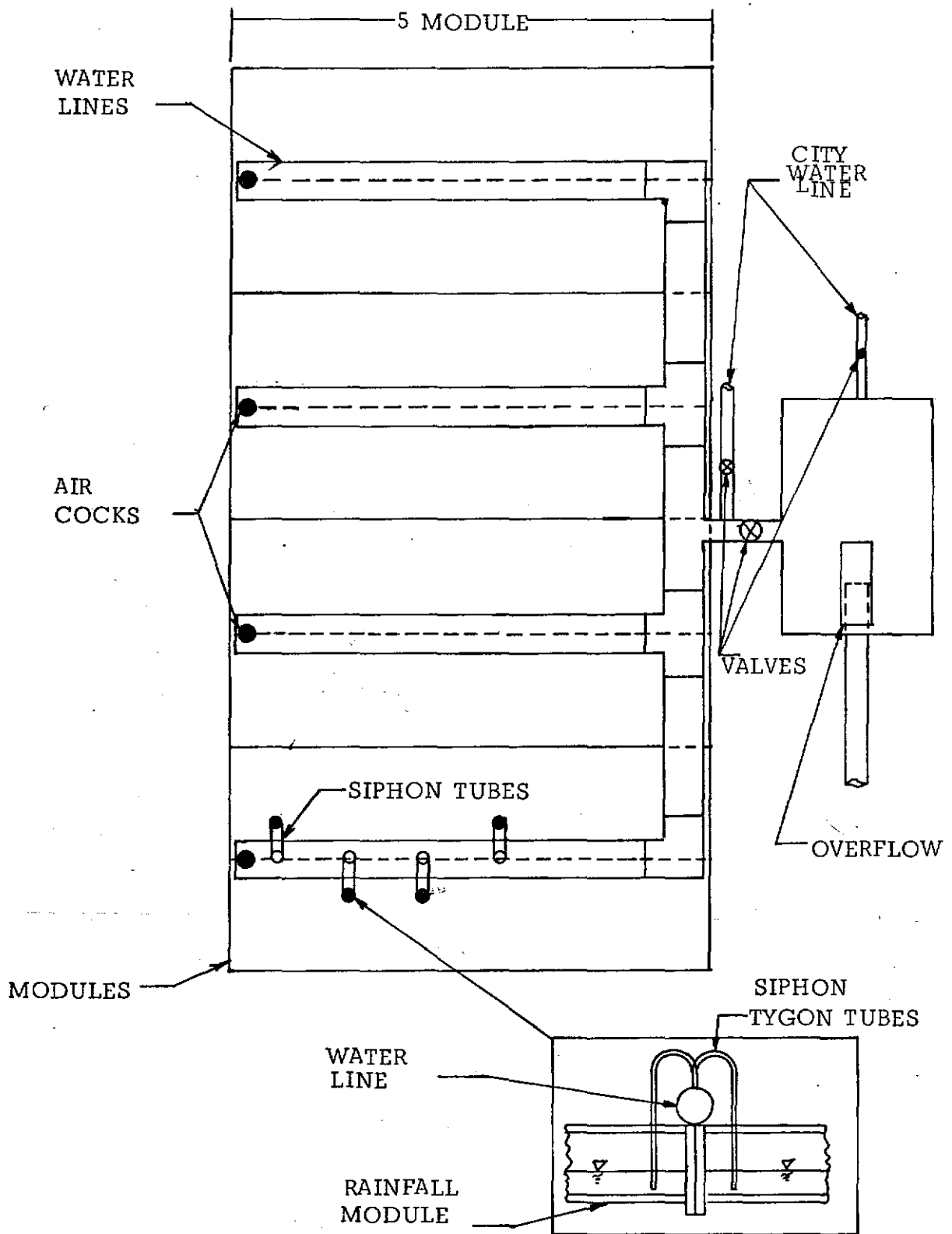


Fig. 6 Water Supply System

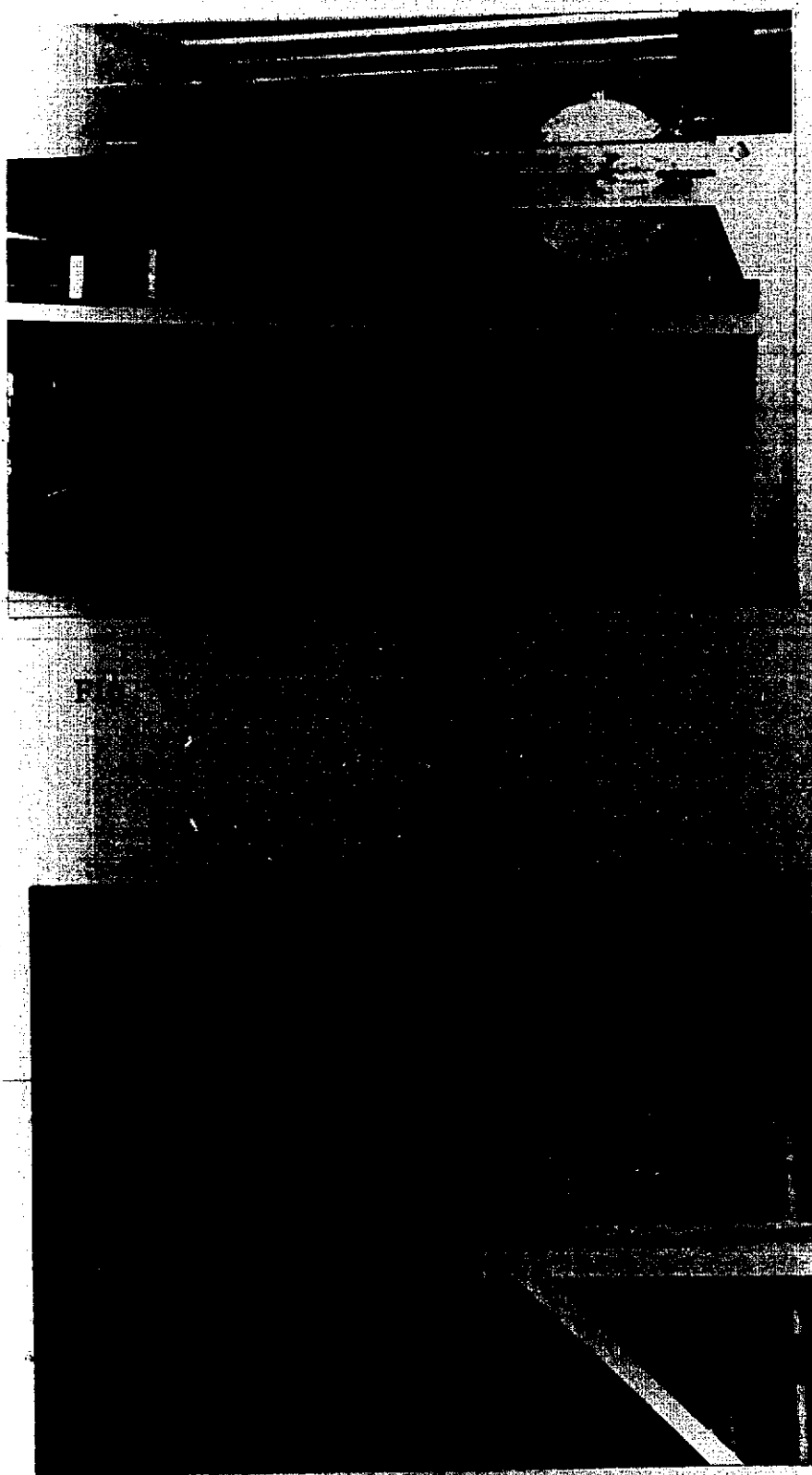


Fig. 8 Constant head tank

of this simulator. The initial velocity is provided by a sudden increase in pressure on top of the water surface. This pressure is larger than the room pressure the bottom surface of the module is exposed to, thus, the drop is ejected from the countersink at the bottom of each hole. This pressure pulse is provided through a rotating valve which is connected by copper tubing air lines to each module and to an air supply reservoir. A schematic drawing of the air supply and pulse control system is depicted as in Fig. 9 and an overall view of the system is shown in Fig. 10.

The rotating air valves as the one shown in Figs. 11 were used to distribute the pressure pulses to the modules. The valve is 10.16 cm (4.0 in) in diameter with a 7.62 cm (3.0 in) diameter rotating core. Compressed air enters the center of the valve and conveys through a 1.27 cm (0.5 in) L shaped duct drilled into the core with one end lining up with the air entrance and the other leg rotating around to permit air to leave each of the ten copper tubes installed on the outside housing. When the rotating L-duct is lined up with a particular air tube, which leads to one of the rainfall modules one pulse is provided to that module and in turn a drop is ejected at each hole on the bottom plate. In the system, four rotating valves were used to provide pulses to the forty modules.

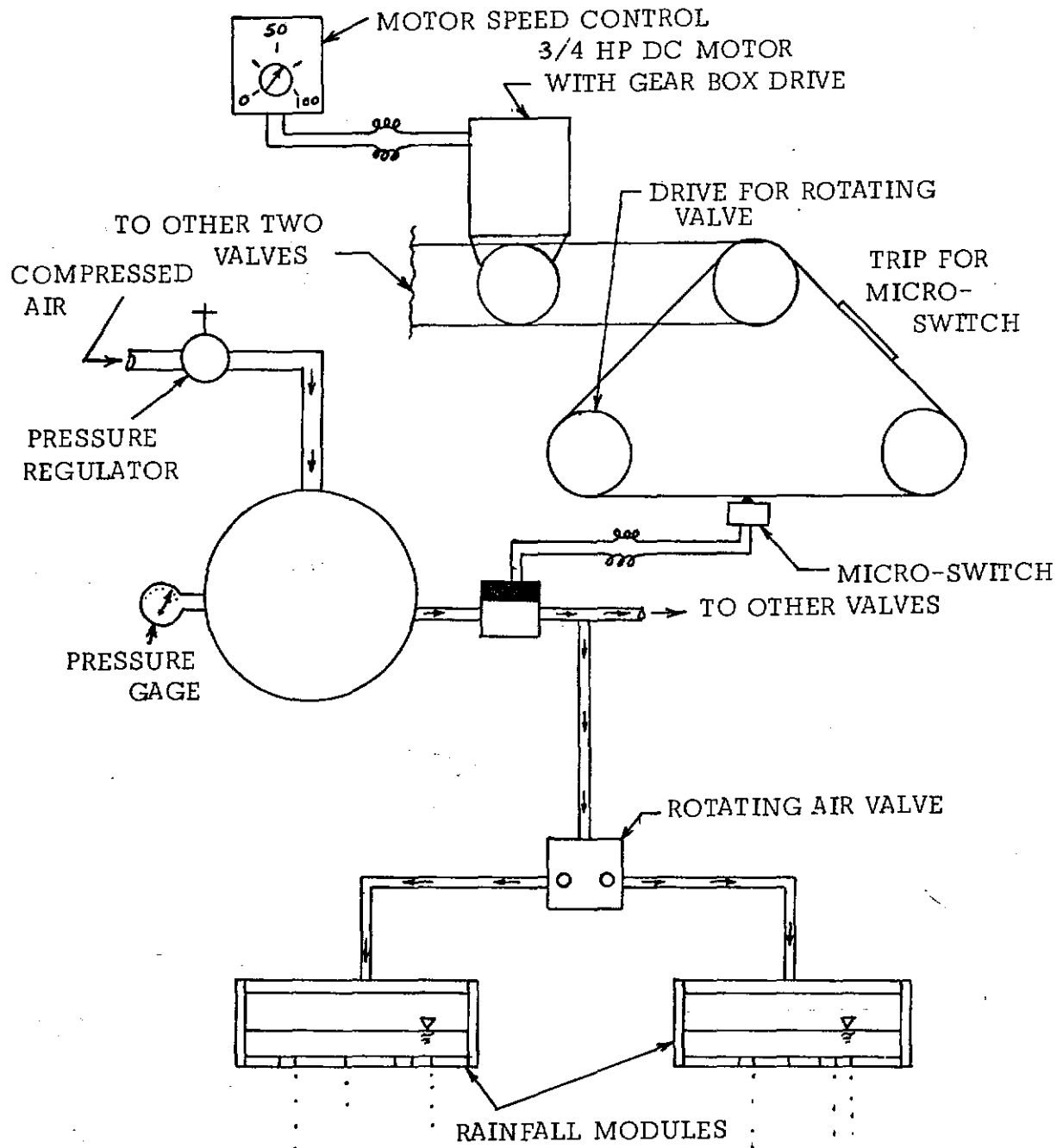


Fig. 9 Schematics of the Pressure Pulse Supply System



Fig. 12 Air distribution system

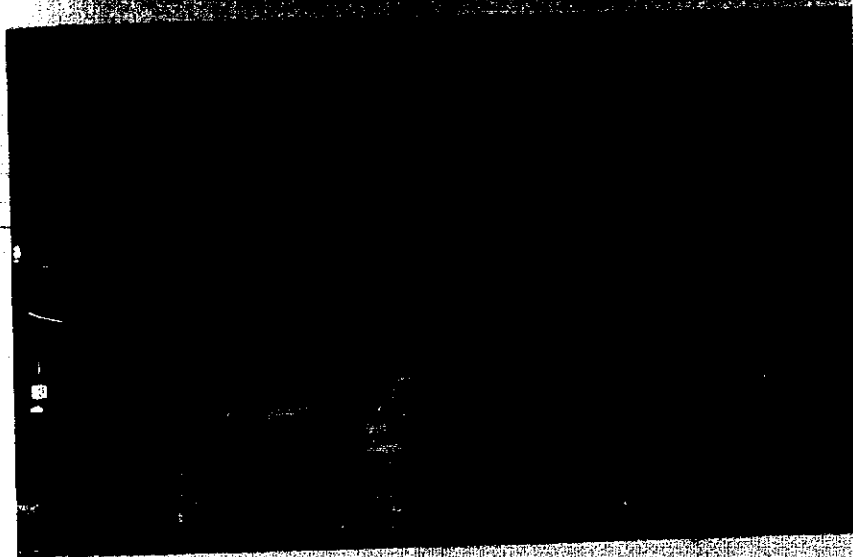


Fig. 13 Pressure pulse distribution valve

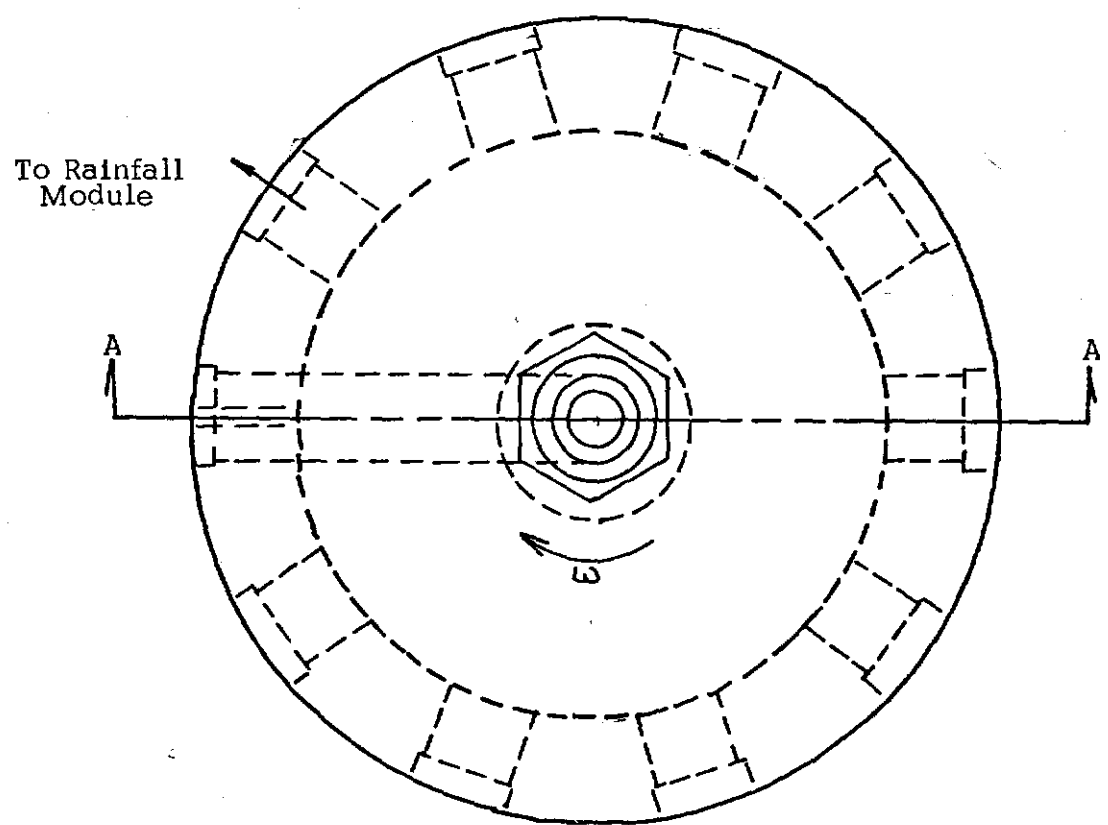
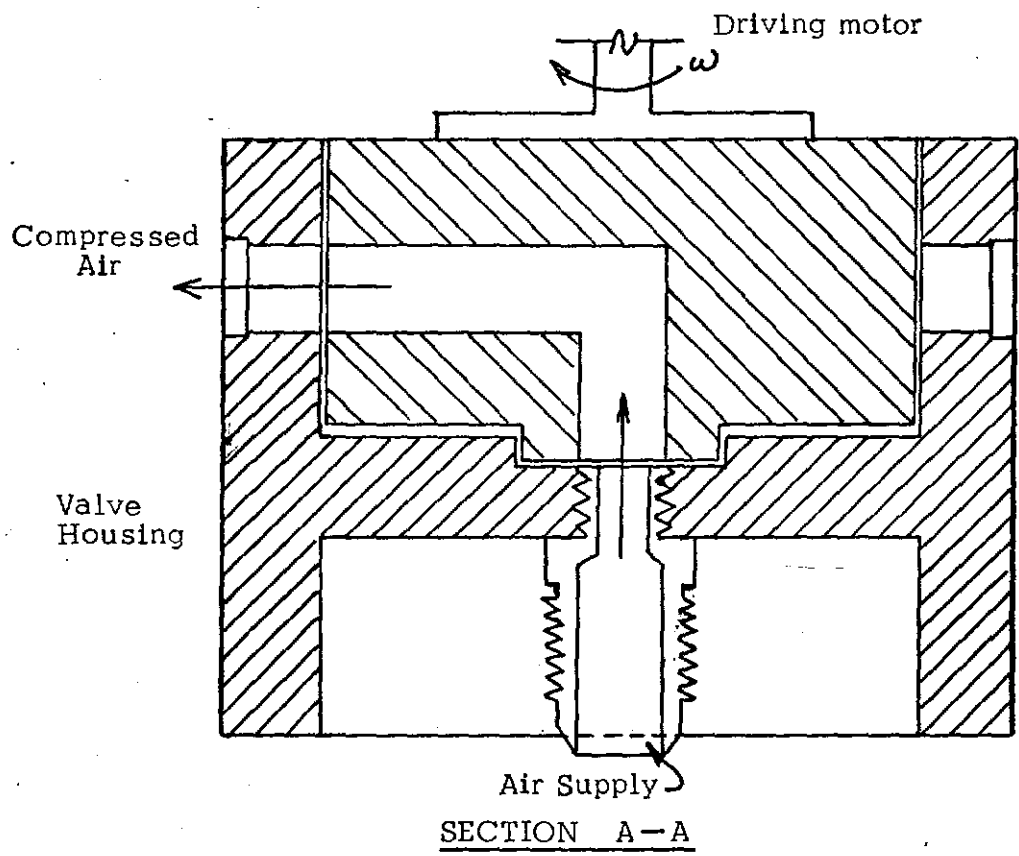


Fig. 11 Rotating Valve for Pressure Pulse Distribution

A V-Belt drive was used to turn the four rotating valves. This system is shown in Fig. 12. Each valve was mounted to a pulley bracket. The entire assembly, rotating valve and pulley bracket, were then mounted on a 1.90 cm (0.75 in) plywood board on 0.61 m (2.0 ft) centers.

A centrally located 3/4 HP DC motor reduction gear box unit with a semetric belt drive was used as the power source to the rotating valves (Fig. 10). To adjust the belt tension a yoke adjustor with a double pulley was used. The belt running through the bottom groove of the pulley in the yoke adjustor turns two rotating valves and the belt through the top grooves transmits the drive from the motor. By using a threaded rod on the adjustor the tension in both belts could be adjusted simultaneously (Fig. 12).

The double pulley on the motor is 15.24 cm (6.0 in) in diameter and those on the yoke adjustor and rotating valve bracket are 7.62 cm (3.0 in). Thus there is a 1:2 ratio of motor gear box speed to rotating valve speed. A reostat control for the motor permits motor speeds to vary from 0 to 356 rpm, so the valve speed can be regulated with a range of 0 to 712 rpm depending on the drop size and intensity desired.

The air lines connecting the rotating valve to the modules are 1.27 cm (0.5 in) copper tubing (Fig. 13). All tubes were cut the same length to avoid any inconsistency in the magnitude of the pulse to each module.

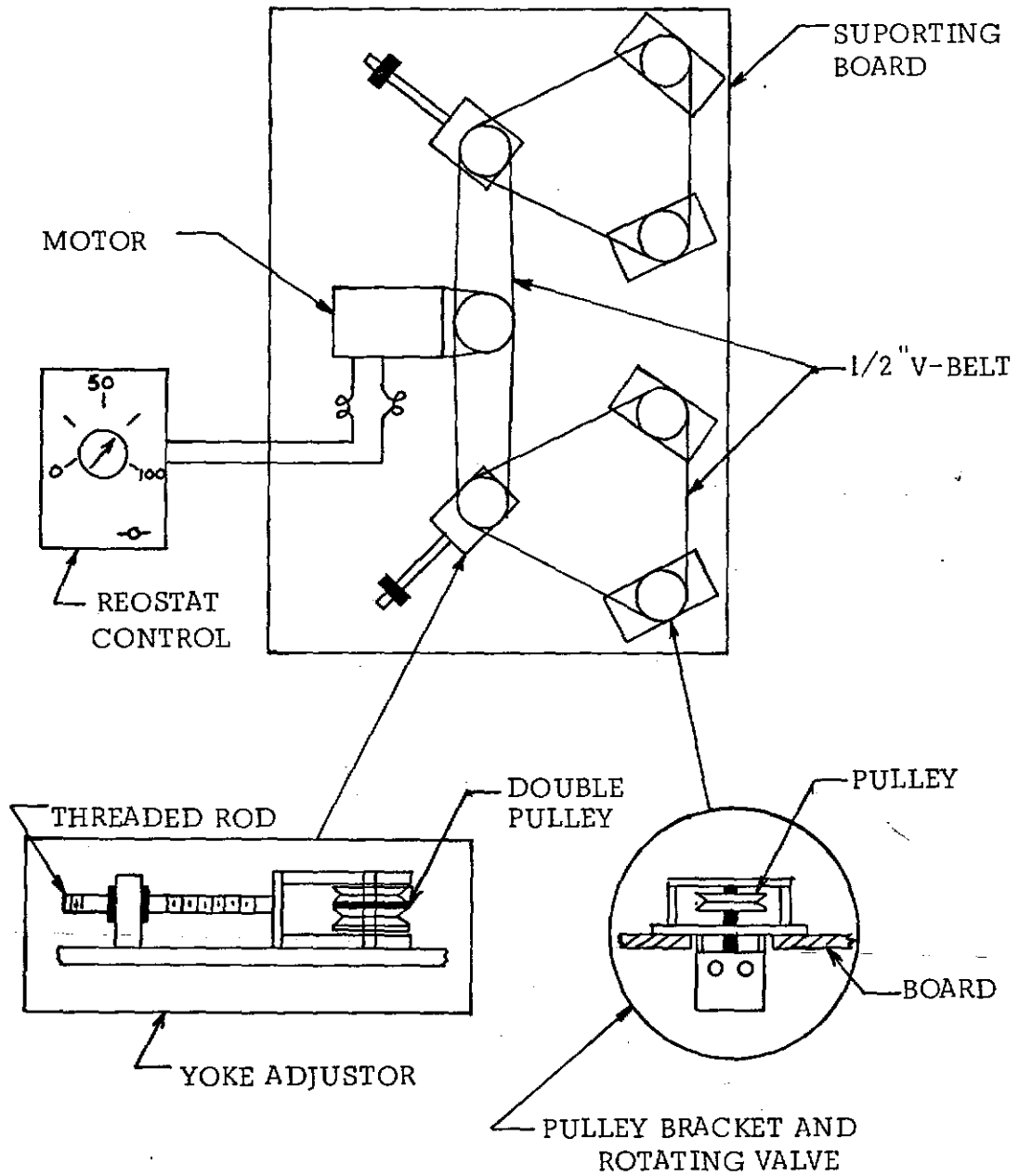


Fig. 12 Rotating Valve Assembly and Speed Control

The air supply reservoir was also mounted to the plywood board as can be seen in Fig. 10. A 1.27 cm (0.5 in) line from the air supply reservoir is connected to a solenoid valve which controls the pressure pulse. On the outlet side of the solenoid valve a line is connected to each of the rotating valves.

The pressure magnitude in the air supply reservoir is controlled by a pressure regulator. A solenoid operated air valve, activated by micro-switches, controls the frequency of air supply from the air supply reservoir (Fig. 9). The micro switches are activated by rubber strips 23.92 cm (9.42 in) long attached to the drive belts which drive the rotating valves. This 23.92 cm (9.42 in) length allows one complete revolution of the air valve, such that when the solenoid valve is activated each module receives a pressure pulse.

The pressure magnitude in the air reservoir controls the speed of air supply into the module while the rotating speed of the valve governs the duration of the supply. The former affects the initial velocity of the drop ejection and the drop size is decided by the latter. Therefore, when they are regulated properly and combined a controlled drop size and velocity variation may be obtained.

The frequency of the pressure pulse is determined by the period of solenoid air valve activation. This is achieved by using different micro switches each operated by rubber strips arranged a different spacing apart.

The availability of the three different adjustments made it possible to control the simulated rainfall. These adjustments made it possible to provide, one desired intensity with frequent small drops or with less frequent large drops. For each drop size the initial velocity can also be controlled to provide the proper amount of kinetic energy during drop splashing. This is particularly desirable due to the need of simulation of water drop impact effect on soil erosion studies. However, due to the complex nature of the unsteady non-uniform flow phenomena during drop formation the relationship between the initial velocity, pressure pulse magnitude and drop size were determined by using empirical methods rather than attempt to solve it analytically.

CHAPTER III

EXPERIMENTAL PROCEDURES

The complex nature of the unsteady nonuniform flow phenomenon which occurred during the pressure pulse-water drop formation period is very difficult, if not impossible to analyze analytically. Therefore, empirical methods were used to test the system in order to determine its rainfall simulation characteristics and to further compute the relative erosivity ratio when the simulator is used as a soil erosion research tool.

Determination of Water Drop Velocity

To determine the water drop velocity, multiple image-photograph method was used. This was done by taking stroboscopic photograph of the falling water drops against a dark background. The most effective lighting arrangement was found, after various trials, to be setting the light beams at an angle approximately 30° from the center line of the camera lens. To provide enough light intensity, three General Radio Company Strobotac Type-A stroboscopes slaved in series, were used. The camera and the stroboscopes were placed outside the pressurized rainfall room. Through the observation windows, a common focus point for

the camera and the strobo light was placed at 7.6 cm (3 in.) in front of the light absorbing dark background, which is set at 152 cm (60 in.) from the film plane. While the scale is attached onto the background screen, the actual waterdrop falling distance would be smaller than that measured using the scale shown on the picture. A correction factor is found by using similar triangle method to be 0.95. The schematic drawing and a photograph of the test arrangement are shown in Figs. 13 and 14 respectively. A picture of the actual water drop image is shown in Fig. 15. The center of the picture is at a distance of approximately 168 cm (5.5 ft.) measured downward from the bottom of the rainfall module.

This picture was taken with the stroboscope set at 3000 flashes per minute and the camera shutter at 1/10 of a second. Therefore, the distance between each two consecutive images of the same water drop was travelled within a time period of 20 ms (0.02 sec). This provides:

$$\text{Drop Velocity} = \frac{\text{Distance}}{0.02} \times 0.95 \quad (1)$$

where 0.95 is the scale factor as stated previously.

This velocity is designated to the distance of fall from the bottom of the rainfall module to the mid-point between these two consecutive images. The velocities elsewhere can then be computed using this velocity and distance of fall. The method of computation will be developed in a later section of this report.

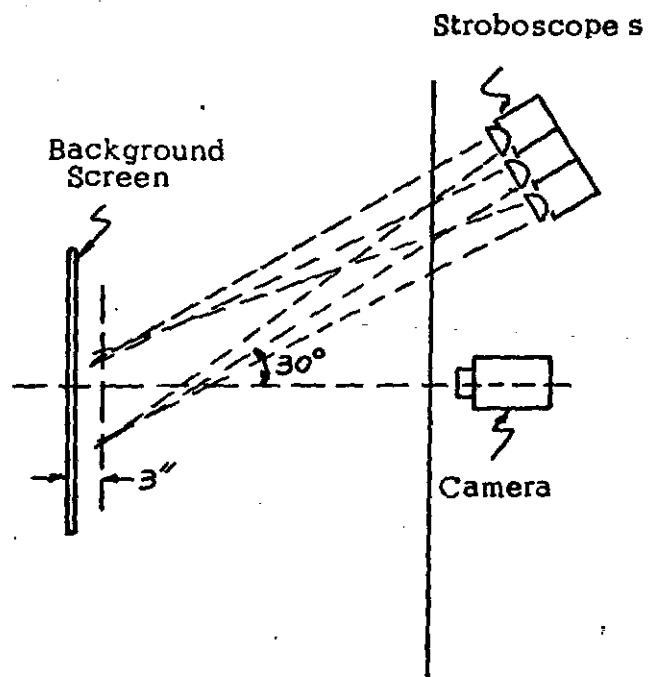
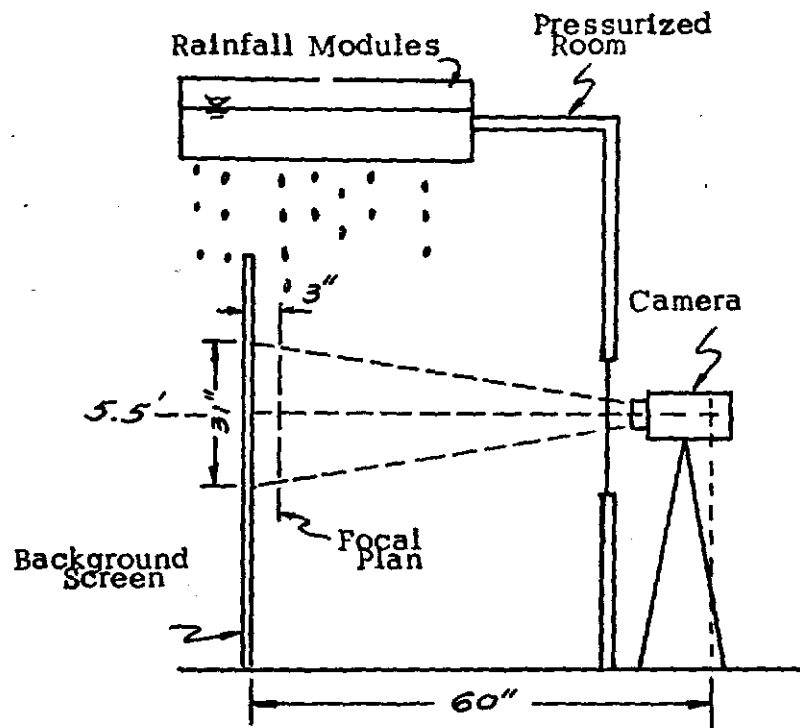
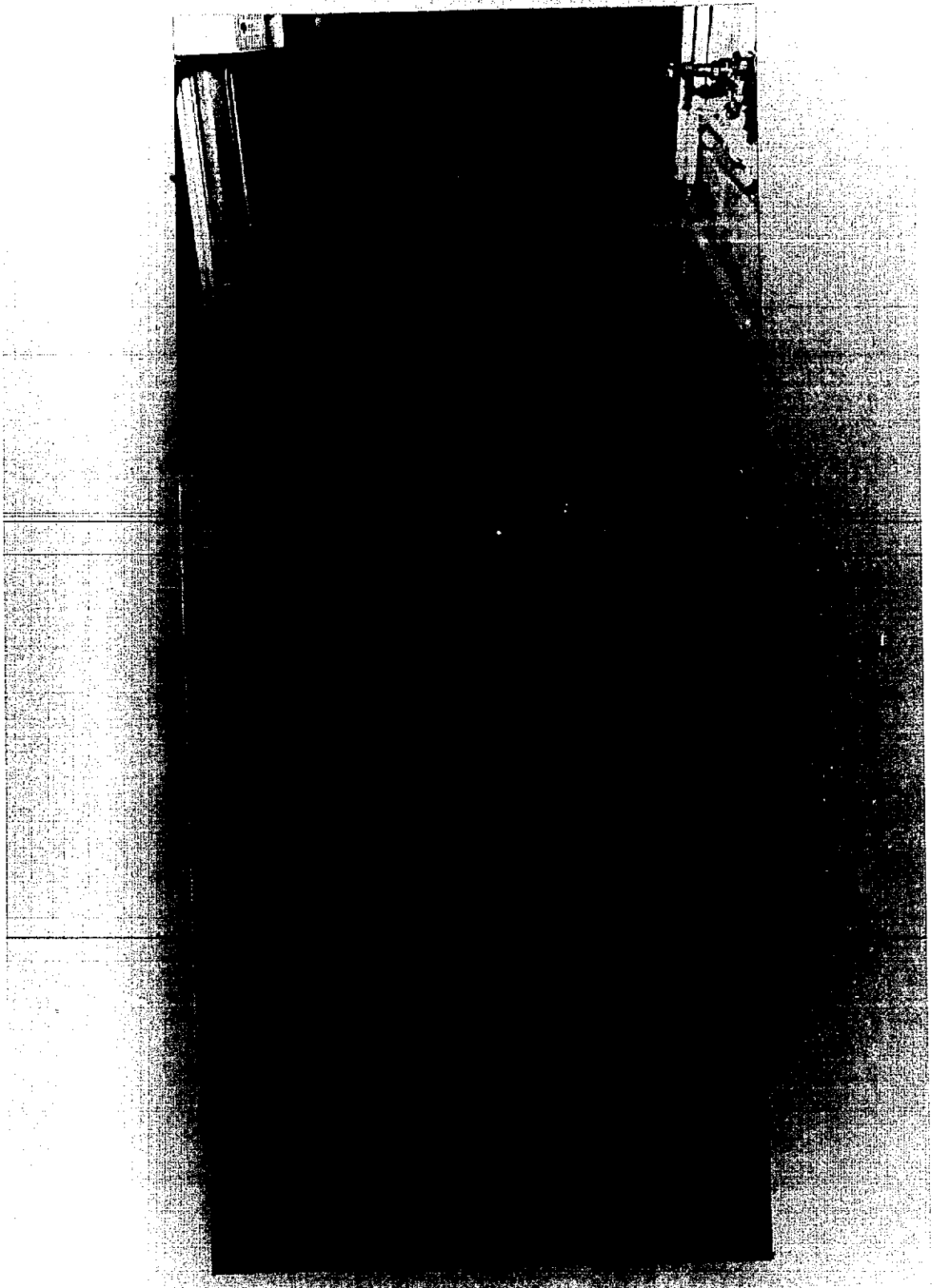


Fig. 13A Drop Velocity Measuring Arrangement



**Fig. 15 Multiple image stroboscopic photograph
for drop size and velocity measurement**

Measurement of Simulated Raindrop Size

Two methods were used to measure the drop size of the simulated rain: direct measurement from the photograph and filter paper method. To measure the drop size directly from the photograph, a micro-mikezox was used. An accuracy of ± 0.01 mm can be obtained by using this method.

The second method makes use of Whatman No. 1 filter paper. When the filter paper was exposed for a short duration of time under the simulated rainfall, each drop striking the filter paper would be absorbed and leaving a permanent stain (Fig. 16). To convert the stain size to drop size an equation determined by Neuman at the Isreal Metreorological Service was employed as follows:

$$d = \left(\frac{D}{3.38} \right)^{2/3} \quad (2)$$

where d = drop diameter in mm

D = stain diameter in mm

Simulated Rainfall Intensity

The intensity was measured by placing container interceptors under the simulated rainfall for known time intervals and measuring the volume of the accumulated water in the container. Several containers were used simultaneously in order to obtain an accurate rainfall intensity measurement.

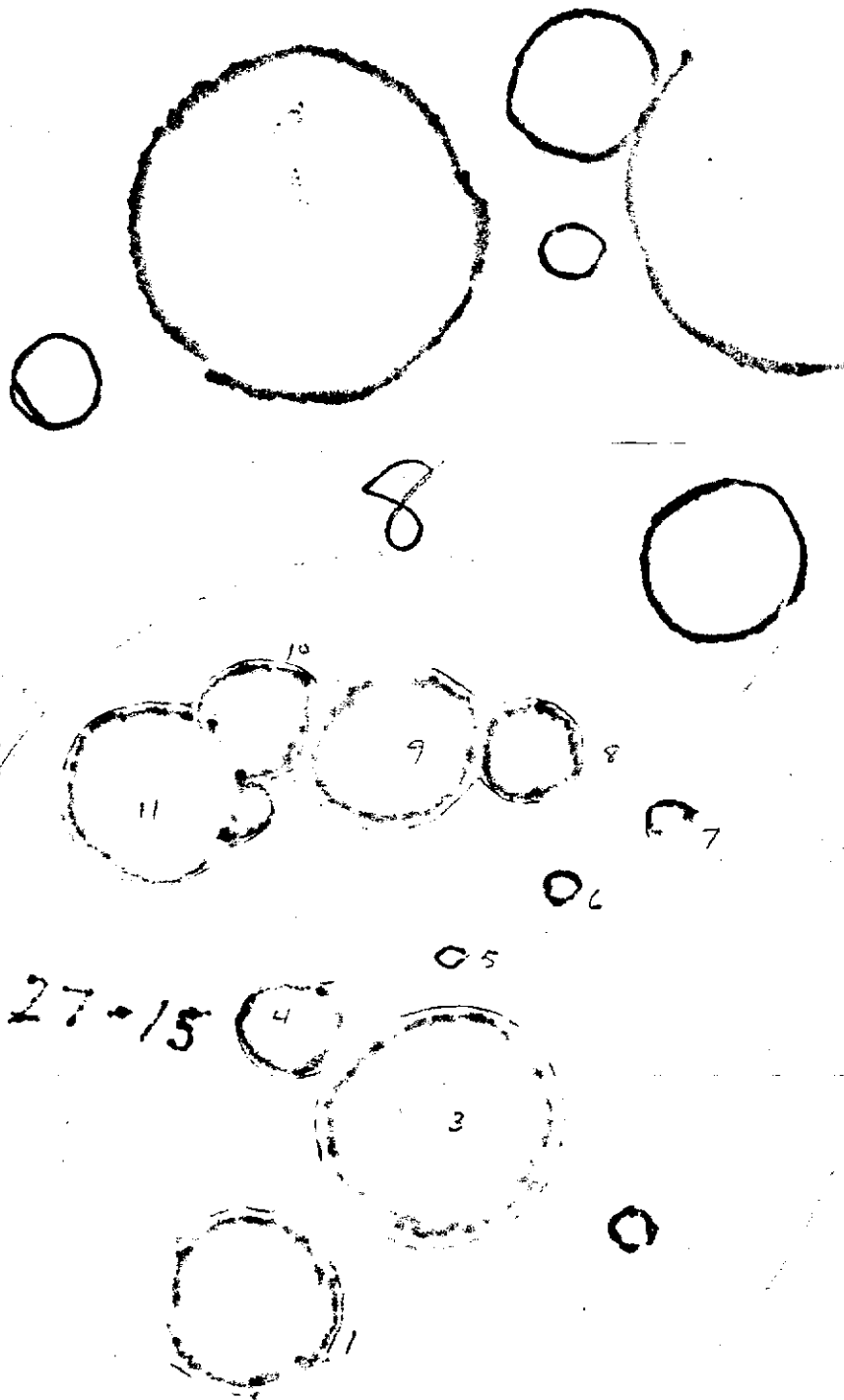


Fig. 16 Drop Stain on Whatman No. 1 Filter Paper

Since this simulator possesses the unique feature of being able to control the rainfall intensity by varying the drop size and/or drop frequency, a total of 35 tests were conducted to produce a range of rainfall intensity from 1.19 to 9.89 in/hr rain. The drop size is controlled by the operating pressure and the valve rotating speed (time duration of pressure pulse application). Higher operating pressure and lower valve rotating speed normally produces larger drop sizes. The drop frequency is controlled by the motor speed and the number of trippings per each revolution of the driving belt. Three tripping arrangements were used. These provides the selection of supplying one, two or three air pressure pulses per each belt revolution and, in turn, determines the drop frequencies.

CHAPTER IV

ANALYSIS OF RESULTS

Derivation of Velocity-Fall Distance Relationships

Considering a spherical water droplet moving through the resisting medium-air, the equation of motion can be written as:

$$F_W - F_D = m \frac{dv}{dt} \quad (3)$$

where F_W = gravitational force acting on the water drop

F_D = drag force due to air resistance

m = mass of the water drop

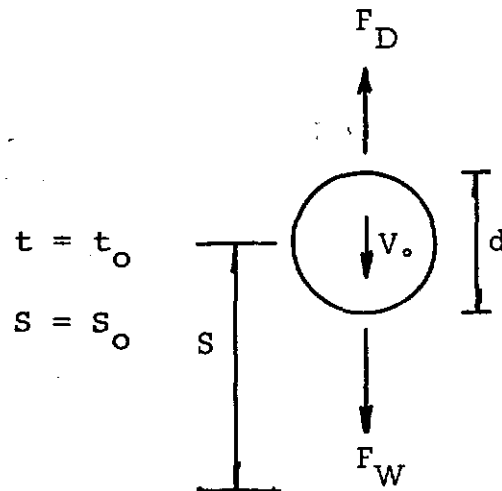


Fig. 17 Definition Sketch of Water Drop Falling Through a Resistive Medium

Using the definition sketch as shown in Fig. 17 and substituting terms, Eq. (3) can be simplified to give:

$$\frac{dv}{dt} = g - \left[\frac{3}{4} \frac{C_d \rho_a}{d \rho_w} \right] v^2 \quad (4)$$

where ρ_a and ρ_w are densities of air and water respectively; g is the gravitational acceleration; d is the drop diameter and C_d is the coefficient of drag, which is a function of the Reynolds number, $R_e = vd/\nu$. For the average simulated rain drop diameter, d , and the velocity range of interest in this study, R_e has a value between 10^3 to 10^4 . This is the region where C_d remains practically constant with a value of 0.4. When the drag coefficient, C_d , is treated as a constant, Eq. (4) can be rewritten as:

$$\frac{g \, dv}{g^2 - r^2 v^2} = dt \quad (5)$$

where

$$r = \sqrt{\frac{3}{4} \frac{C_d \rho_a}{d \rho_w} \cdot g} \quad (6)$$

Integrating Eq. (5) and applying the initial condition, $v = V_0$ at $t = 0$, yield:

$$\frac{1 + (r/g) \frac{v}{V_0}}{1 - (r/g) \frac{v}{V_0}} = \Lambda e^{2rt} \quad (7)$$

where

$$\Lambda = \frac{1 + (r/g) v_0}{1 - (r/g) v_0} \quad (8)$$

This gives the velocity of the water drop at anytime, t , as:

$$v = \frac{ds}{dt} = -\frac{g}{r} \frac{1 - \Lambda e^{2rt}}{1 + \Lambda e^{2rt}} \quad (9)$$

Further integration of the above equation gives:

$$s = \frac{g}{r^2} \log_e (e^{-rt} + \Lambda e^{rt}) + C \quad (10)$$

When the initial condition, $s = s_0$ at $t = 0$ is applied, Eq. (10) becomes:

$$s - s_0 = \Delta s = \frac{g}{r^2} \log_e \left[\frac{e^{-rt} + \Lambda e^{rt}}{1 + \Lambda} \right] \quad (11)$$

or

$$(1 + \Lambda) e^{\left[\frac{\Delta s r^2}{g} \right]} = e^{-rt} + \Lambda e^{rt} \quad (12)$$

Solving for t as a function of Δs yields:

$$t = \frac{1}{r} \log_e \left[\frac{\phi + \sqrt{\phi^2 - 4 \Lambda}}{2 \Lambda} \right] \quad (13)$$

where

$$\phi = (1 + \Lambda) e^{\left[\frac{\Delta s r^2}{g} \right]} \quad (14)$$

Equation (13) gives the time in second for a certain water drop of diameter, d , with an initial velocity, V_0 , to fall a distance, ΔS , while still accelerating. In computing t only positive sign provides a physically realistic solution. The velocity at the end of the fall can be calculated by using Eq. (9).

The actual computation of the numerous data points was carried out by a digital computer. A sample of the computer output, which lists the computed drop diameter, measured velocity, distance where the velocity was measured and the computed initial velocity and velocities of the same drop at 8, 10 and 12 ft. of fall, is shown in Table I. The velocity of natural rain drop of the same diameter is also computed using the data presented by Laws(17) and Gunn and Kinzer (18). Their data were plotted on a semilogarithmic paper as shown in Fig. 18 and fitted with an equation as:

$$V_n = 4.04 + 3.55 (\text{Log}_e d) \quad (15)$$

in which V_n is the terminal velocity in meter per second of the drop of diameter d (mm). The calculated simulated rain drop velocity of test run No. 34 (Table I) is also plotted in Fig. 18 for comparison.

The mean diameter of a given natural rainfall intensity is computed from information presented by Laws and Parsons (20). This diameter is also input to the

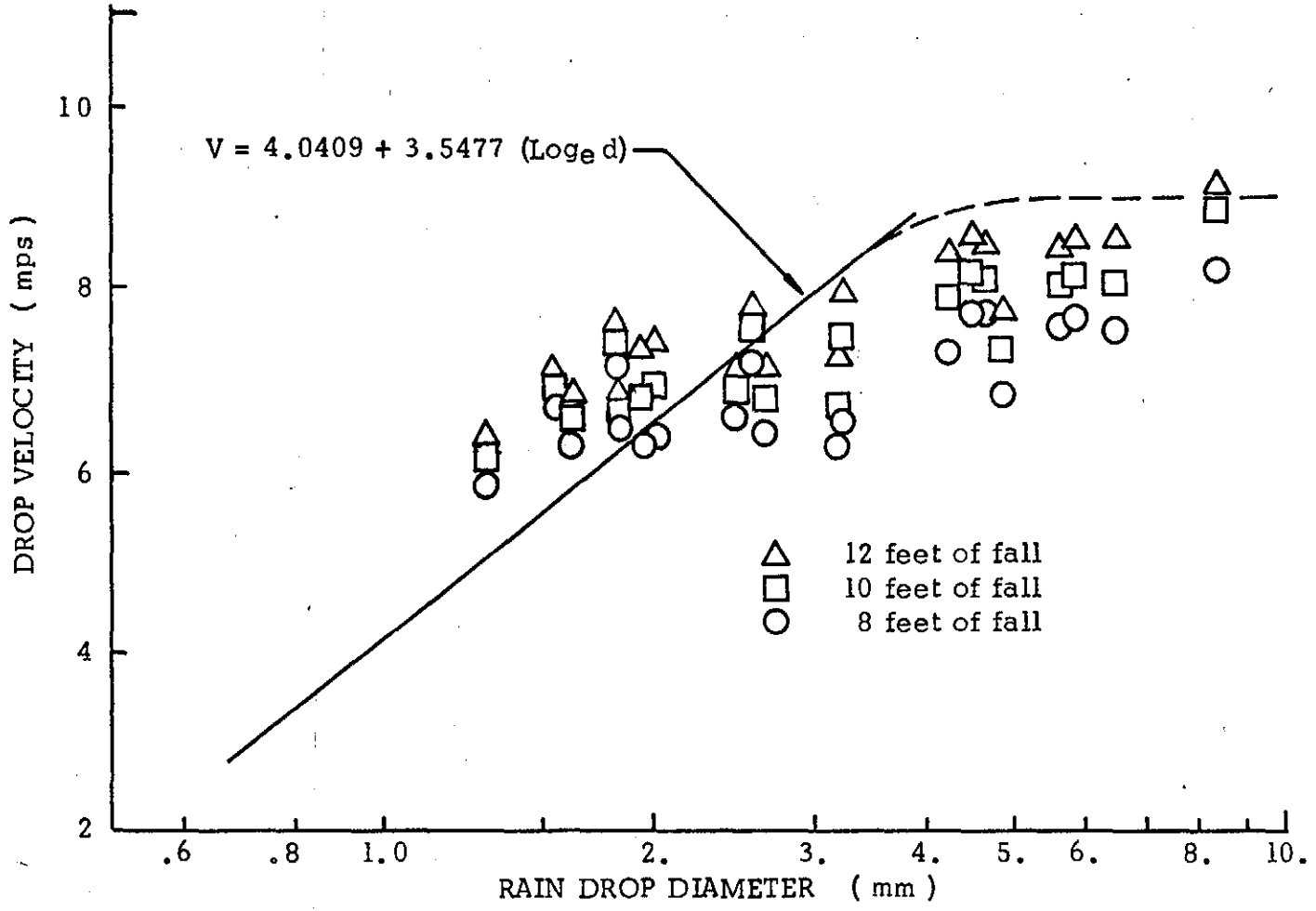


Fig. 18 Relationship Between Rain Drop Diameter and Fall Velocity

TABLE I DROP VELOCITY COMPUTATION

THESE COMPUTATIONS ARE FOR THE DATA OF RUN NO. 34

DROP DIAM (MM)	MEASURED VELOCITY		DISTANCE AT MEASUREMENT		COMPUTED VELOCITIES AT				VELOCITY OF NAT. RAIN	
	(FPS)	(MPS)	(FT)	(M)	0 FT (FPS)	8 FT (FPS)	10 FT (FPS)	12 FT (FPS)	(FPS)	(MPS)
4.57	23.26	7.09	5.00	1.52	18.05	25.43	26.63	27.68	29.50	8.99
4.57	22.76	6.94	4.70	1.43	17.65	25.24	26.47	27.53	29.50	8.99
4.89	19.79	6.03	5.53	1.69	9.95	22.37	24.08	25.54	29.50	8.99
2.61	21.28	6.48	5.63	1.72	16.33	22.53	23.38	24.06	25.61	7.81
8.48	23.75	7.24	4.71	1.44	17.77	26.84	28.44	29.88	29.50	8.99
1.96	19.79	6.03	5.46	1.66	15.56	20.87	21.49	21.98	22.26	6.79
1.96	21.77	6.64	4.92	1.50	20.13	22.39	22.68	22.91	22.26	6.79
3.26	23.26	7.09	5.57	1.70	18.83	24.54	25.41	26.14	28.20	8.60
6.52	22.27	6.79	5.46	1.66	14.53	24.72	26.37	27.82	29.50	8.99
5.87	22.76	6.94	5.06	1.54	16.39	25.34	26.82	28.12	29.50	8.99
4.57	23.75	7.24	5.05	1.54	18.79	25.79	26.95	27.95	29.50	8.99
3.26	20.78	6.33	5.10	1.56	14.80	22.88	24.02	24.97	28.20	8.60
2.61	22.76	6.94	5.08	1.55	19.74	23.88	24.47	24.97	25.61	7.81
5.87	22.56	6.88	5.02	1.53	16.12	25.21	26.71	28.02	29.50	8.99
1.63	20.58	6.27	5.16	1.57	19.36	20.95	21.14	21.27	20.14	6.14
1.63	21.77	6.64	5.30	1.62	21.77	21.77	21.77	21.77	20.14	6.14
2.61	20.19	6.15	4.74	1.45	15.32	22.17	23.08	23.82	25.61	7.81
1.96	20.58	6.27	4.89	1.49	17.83	21.59	22.05	22.41	22.26	6.79
1.96	20.58	6.27	5.29	1.61	17.51	21.48	21.97	22.35	22.26	6.79
1.30	20.58	6.27	5.08	1.55	20.58	20.58	20.58	20.58	17.54	5.35

computer program for computing the ratio of the simulated rainfall diameter to that of natural rain of the same intensity, $[\bar{D}_s/\bar{D}_n]$. The computer was further instructed to determine the relative erosivity of the simulated rainfall by using the relationship suggested by Meyer (21):

$$\text{Relative Erosivity} \approx \left[\frac{\bar{D}_s}{\bar{D}_n} \right]^a \left[\frac{\bar{V}_s}{\bar{V}_n} \right]^b \quad (16)$$

where $a = 1$ and $b = 1$ for momentum relationship and $b = 2$ for kinetic energy relationship. A sample results is presented in Table II.

Rainfall Simulator Characteristics

A total of 35 experimental runs were conducted to test the newly developed rainfall simulator. The test data are presented in Table III and plotted in Fig. 19 as rainfall intensity vs operating pressure. Figure 19 indicates, as expected, that greater operating pressure produces larger intensity rain. For the same operating pressure more frequent drops generally yield higher rainfall intensity.

The mean drop diameter for each simulated rainfall intensity is plotted in Fig. 20. Also shown in Fig. 30 is the curve interpolated from Laws' data (20) representing the average drop size for natural rainfall.

TABLE II RELATIVE EROSIVITY COMPUTATION

DROP DIAM	VELOCITY OF NAT. RAIN		MOMENTUM RATIO			KINETIC E. RATIO (SQUARE OF)		
	(MM)	(FPS)	(MPS)	(V8/VN)	(V10/VN)	(V12/VN)	(V8/VN)	(V10/VN)
4.57	29.50	8.99	0.862	0.903	0.938	0.743	0.815	0.880
4.57	29.50	8.99	0.856	0.897	0.933	0.732	0.805	0.871
4.89	29.50	8.99	0.758	0.816	0.866	0.575	0.666	0.750
2.61	25.61	7.81	0.880	0.913	0.940	0.774	0.833	0.883
8.48	29.50	8.99	0.910	0.964	1.013	0.828	0.929	1.026
1.96	22.26	6.79	0.937	0.965	0.987	0.879	0.932	0.975
1.96	22.26	6.79	1.006	1.019	1.029	1.011	1.038	1.059
3.26	28.20	8.60	0.870	0.901	0.927	0.757	0.812	0.859
6.52	29.50	8.99	0.838	0.894	0.943	0.702	0.799	0.889
5.87	29.50	8.99	0.859	0.909	0.953	0.738	0.827	0.909
4.57	29.50	8.99	0.874	0.913	0.948	0.764	0.834	0.898
3.26	28.20	8.60	0.811	0.852	0.885	0.658	0.725	0.784
2.61	25.61	7.81	0.932	0.956	0.975	0.869	0.913	0.950
5.87	29.50	8.99	0.855	0.905	0.950	0.731	0.820	0.902
1.63	20.14	6.14	1.040	1.050	1.056	1.082	1.101	1.116
1.63	20.14	6.14	1.081	1.081	1.081	1.169	1.169	1.169
2.61	25.61	7.81	0.866	0.901	0.930	0.750	0.813	0.865
1.96	22.26	6.79	0.970	0.991	1.007	0.940	0.981	1.014
1.96	22.26	6.79	0.965	0.987	1.004	0.931	0.974	1.008
1.30	17.54	5.35	1.173	1.173	1.173	1.377	1.377	1.377
THE AVERAGE MOMENTUM RATIO (V8/VN) IS: 0.917						EROSIVITY IS : 0.87		
THE AVERAGE MOMENTUM RATIO (V10/VN) IS : 0.949						EROSIVITY IS : 0.90		
THE AVERAGE MOMENTUM RATIO (V12/VN) IS : 0.977						EROSIVITY IS : 0.93		
THE AVERAGE KINETIC ENERGY RATIO (V8/VN)**2 IS: 0.851						EROSIVITY IS : 0.81		
THE AVERAGE KINETIC ENERGY RATIO (V10/VN)**2 IS: 0.908						EROSIVITY IS : 0.86		
THE AVERAGE KINETIC ENERGY RATIO (V12/VN)**2 IS: 0.959						EROSIVITY IS : 0.91		
THE SIMULATED RAINFALL INTENSITY IS : 4.97 IN/HR								
THE MEAN DROP DIAMETER OF LIKE NATU. RAIN IS : 3.30 MM								
THE AVERAGE INITIAL VELOCITY IS : 17.35 FPS OPERATING PRESSURE IS : 15.00 PSIG								
THE MEAN DIAM. OF THE SIMU. RAIN (USING BOTH PHOTO. AND FILT. PAPER) IS : 3.14 MM								

TABLE III SIMULATED RAINFALL DATA

RUN NO.	OP PRESS (psi)	DROP FREQUENCY (Drops/Sec)	RAINFALL INTENSITY (in/hr)	AVERAGE DROP SIZE	
				SIMULATOR (mm)	NATURE (mm)
1	2.4	0.70	1.19	2.80	2.07
2	2.0	2.80	1.89	3.22	2.30
3	1.6	6.28	1.39	2.37	2.15
4	4.0	2.10	1.21	2.97	2.05
5	4.5	2.80	1.43	3.07	2.30
6	4.5	3.50	3.92	2.89	2.90
7	4.6	0.96	2.18	2.81	2.35
8	4.6	3.85	2.64	3.17	2.55
9	6.0	0.62	3.08	3.83	2.70
10	6.0	2.45	3.16	3.40	2.70
11	6.0	5.49	4.84	3.86	3.15
12	6.0	0.79	3.06	2.67	2.65
13	6.0	3.15	3.27	2.56	2.60
14	6.0	7.07	4.23	2.75	3.00
15	6.5	2.94	2.66	3.57	2.70
16	6.5	6.59	6.60	4.03	3.95
17	7.0	2.80	3.98	3.25	2.95
18	7.0	3.50	4.70	3.41	3.10
19	8.0	0.73	2.09	2.97	2.35
20	8.0	2.80	3.52	3.57	2.75
21	8.0	4.20	4.87	2.43	3.15
22	8.0	4.90	4.84	2.84	3.15
23	8.5	7.46	5.85	3.89	3.70
24	8.5	0.83	2.87	3.17	2.55
25	9.0	3.32	3.67	3.97	3.20
26	10.0	0.70	5.16	3.40	3.40
27	10.0	0.83	2.58	3.67	2.48
28	11.0	7.46	9.89	3.86	4.40
29	12.0	2.80	6.76	3.44	3.95
30	12.0	3.32	3.79	2.65	2.88
31	12.0	7.46	6.76	2.27	3.95
32	15.0	6.28	7.38	3.09	4.00
33	15.0	2.80	6.57	2.94	3.80
34	15.0	0.70	4.97	3.14	3.30
35	16.0	0.83	6.20	2.35	3.80

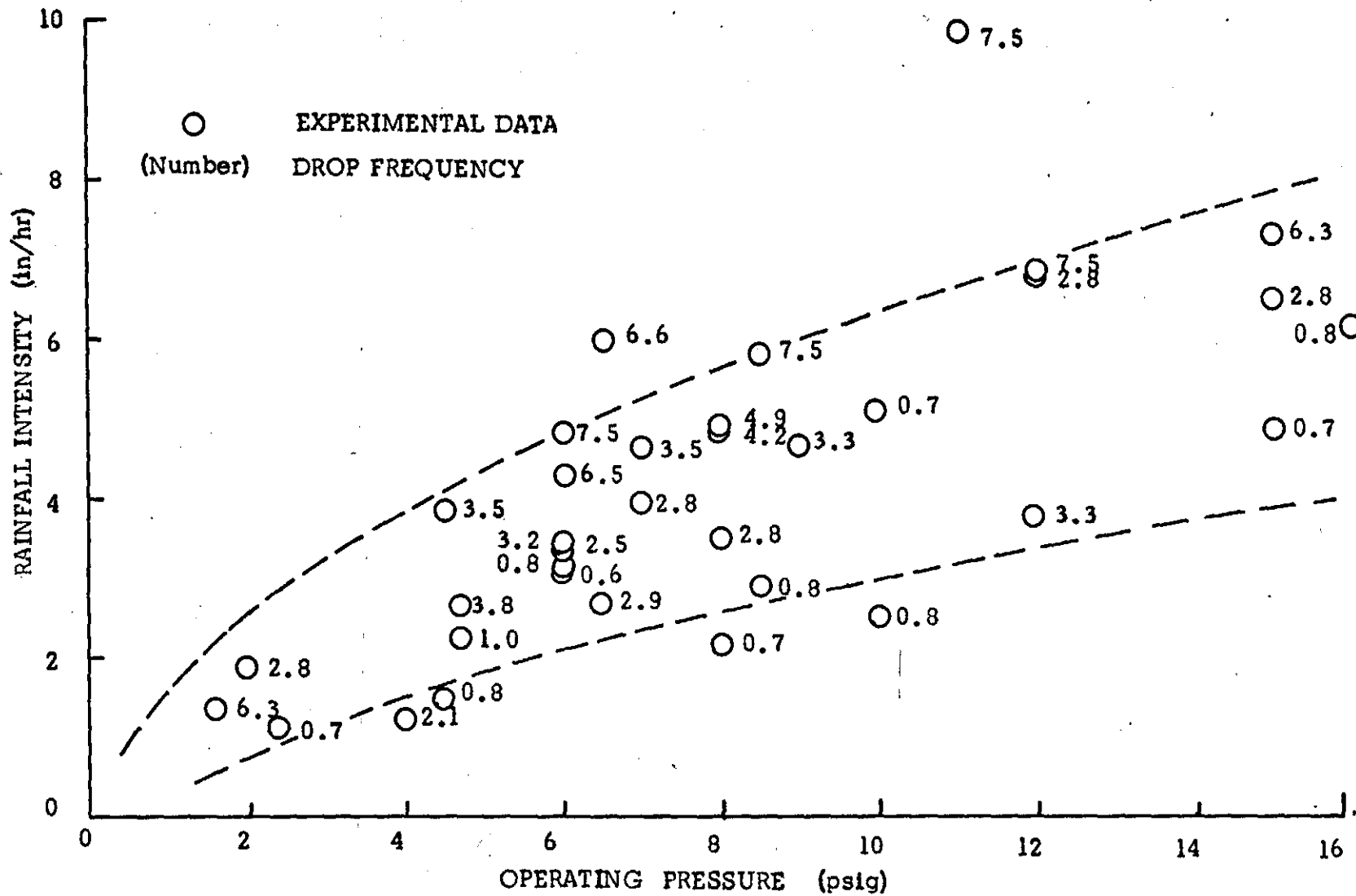


Fig. 19 Rainfall Simulator Operation Characteristics

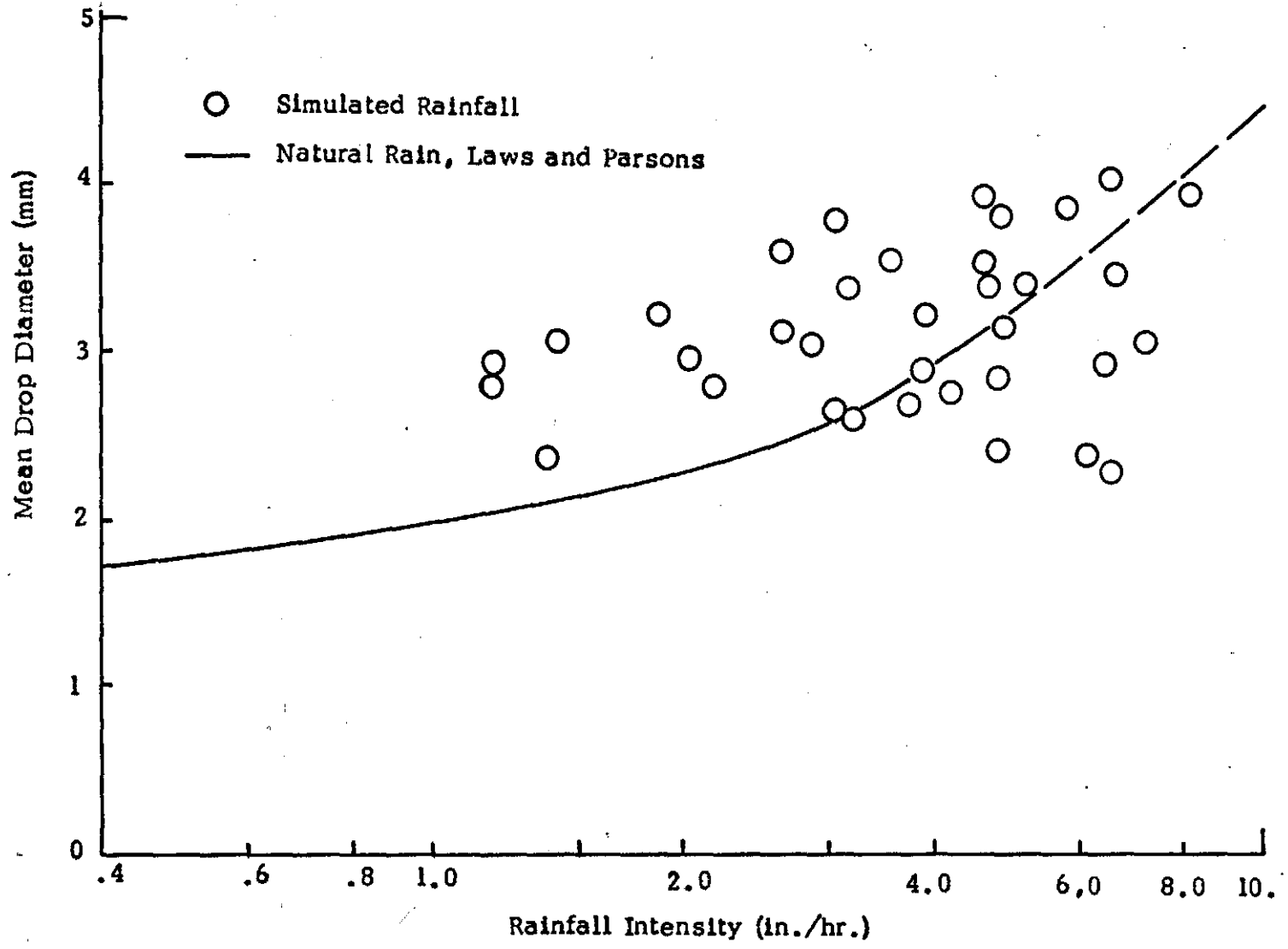


Fig. 20 Rainfall Intensity and Drop Diameter Relationship

Relative Erosivity Ratio

As described in the previous section relative erosivity ratio can be computed in two different ways; by using momentum or kinetic energy relationship. The selection of the one from the other are often based on the researcher's preference (21). However, for a good rainfall simulation, which provides the velocity ratio of the simulated to the natural rain near unity, either method of computation should produce satisfactory results in erosivity simulation provided that diameter ratio, (\bar{D}_s/\bar{D}_n) , are also near unity. Table IV listed the computer results using both momentum and kinetic energy relationships. An average of 86% at 8 ft. (2.44 m) to 102% at 12 ft. (3.66 m) of fall distance are noted for momentum simulation. For kinetic energy simulation, a mean value of 70% to 91% is obtained at the same distances of fall. Three plots were made to show the relative erosivity of the simulated rainfall at 8, 10 and 12 ft (2.44, 3.05 and 3.66 m) of fall. These are shown in Figs. 21, 22 and 23 respectively.

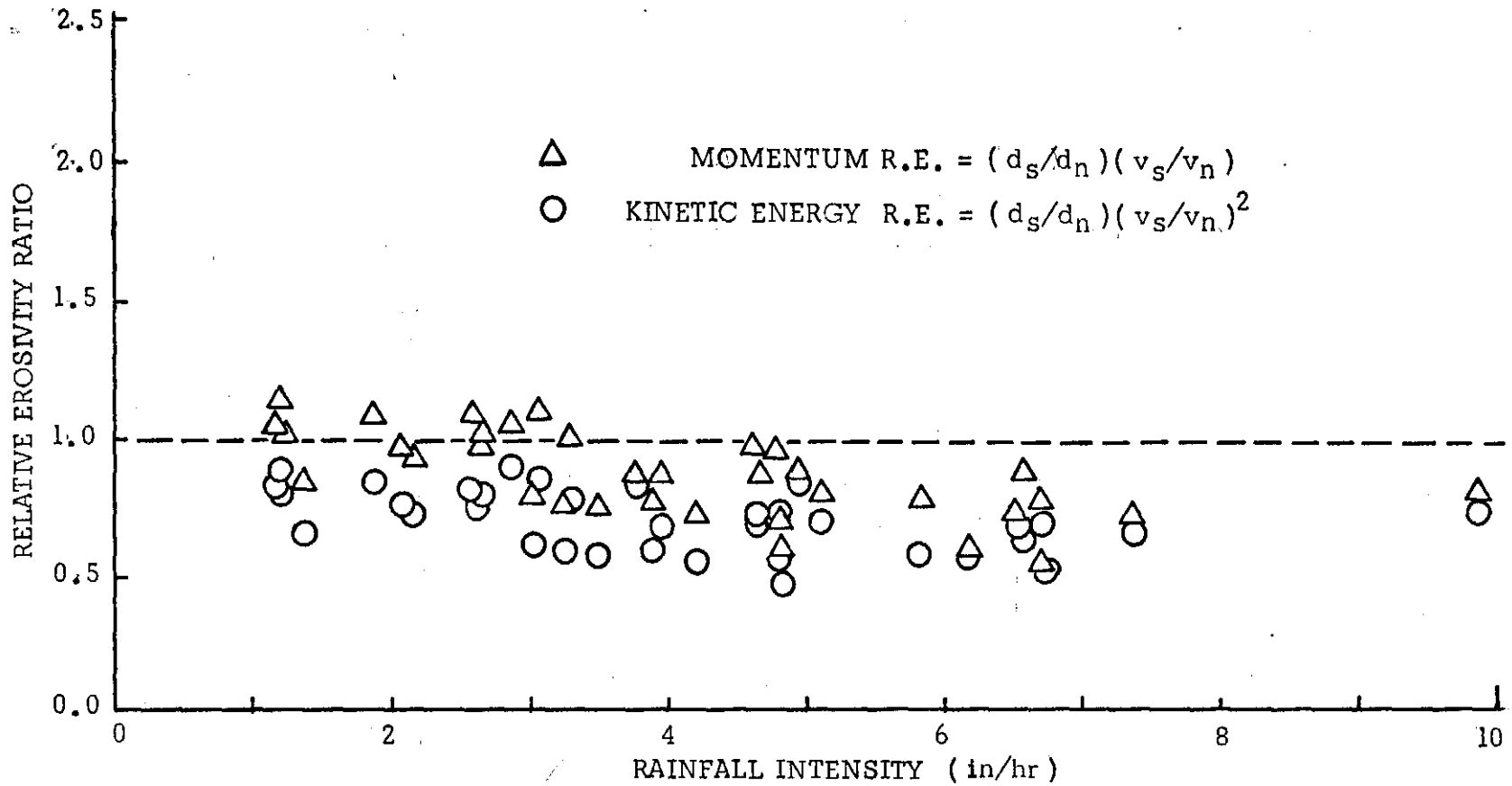


Fig. 21 Relative Erosivity Ratio of the Simulated Rainfall at Eight Feet of Fall

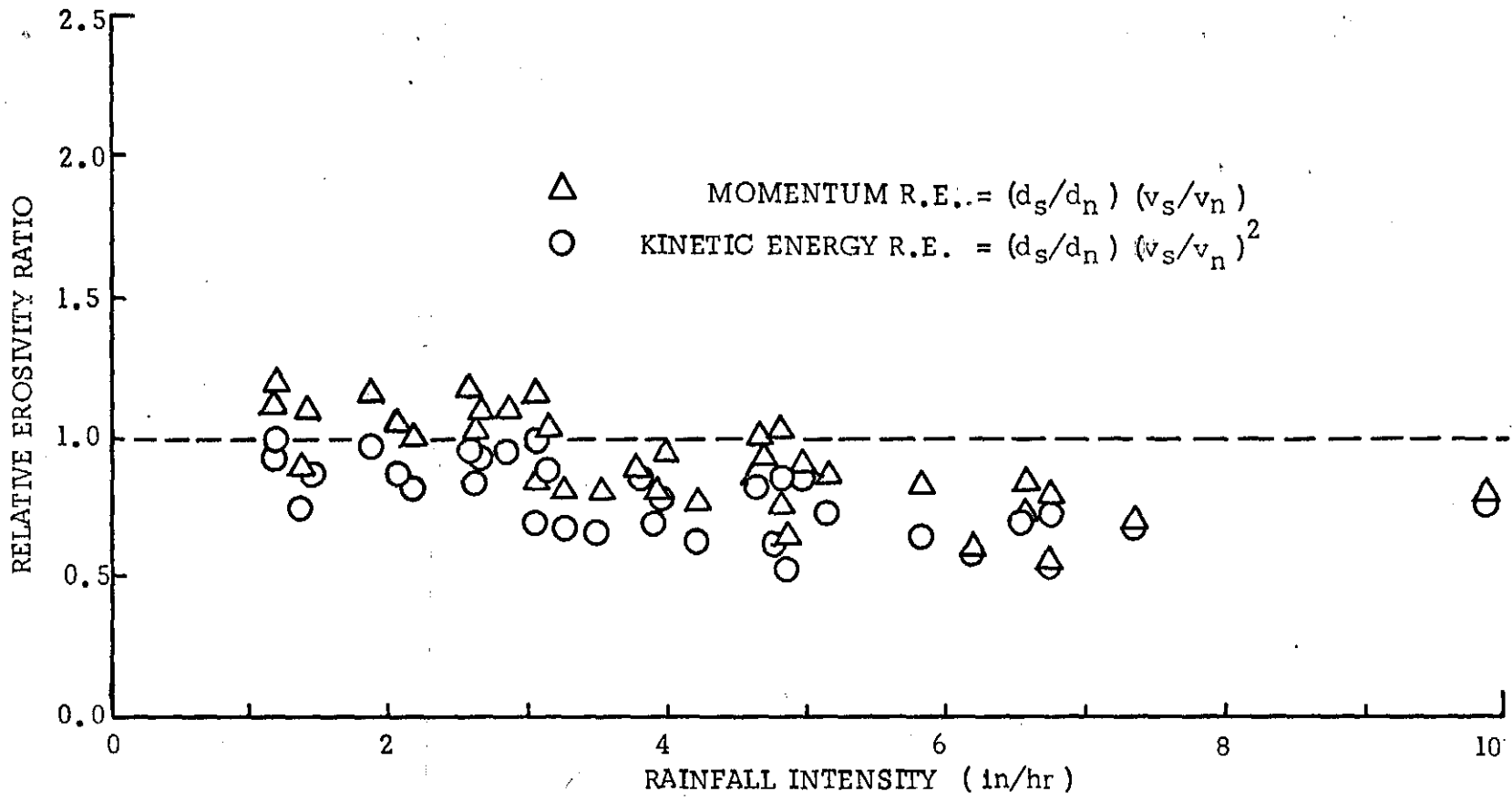


Fig. 22 Relative Erosivity Ratio of the Simulated Rainfall at Ten Feet of Fall

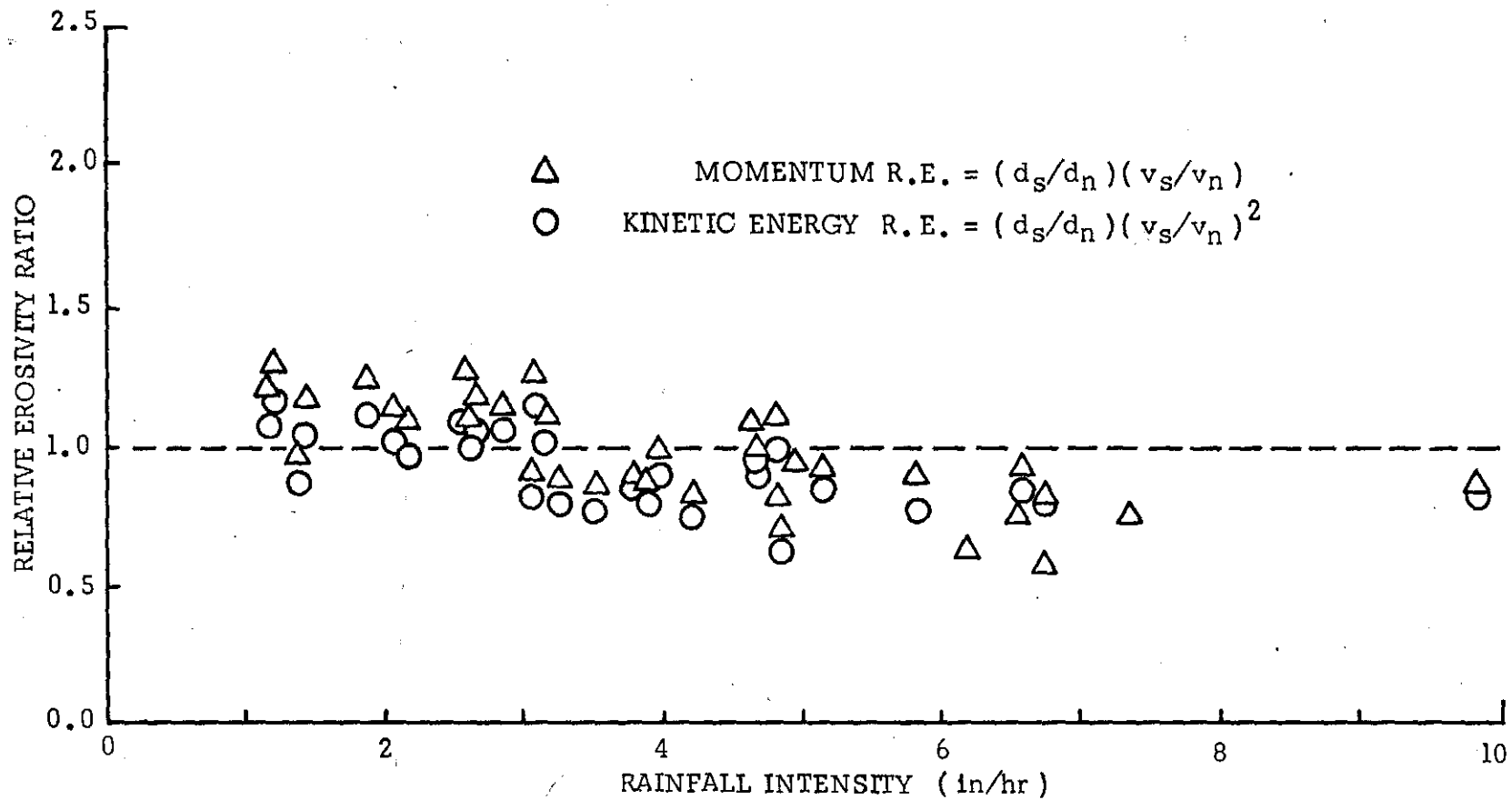


Fig. 23 Relative Erosivity Ratio of the Simulated Rainfall at Twelve Feet of Fall

TABLE IV RELATIVE EROSIVITY RATIO

RUN NO.	RAINFALL INTENSITY (In/Hr)	RATIO OF AVE. DIAM.	RELATIVE EROSIVITY RATIO OF MOMENTUM			RELATIVE EROSIVITY RATIO OF K.E.		
			V_8/V_N	V_{10}/V_N	V_{12}/V_N	V_8/V_N	V_{10}/V_N	V_{12}/V_N
1	1.19	1.35	1.04	1.13	1.20	0.81	0.94	1.07
2	1.89	1.40	1.08	1.17	1.24	0.83	0.98	1.11
3	1.39	1.10	0.84	0.91	0.97	0.64	0.75	0.86
4	1.21	1.45	1.12	1.21	1.29	0.87	1.0.	1.15
5	1.43	1.33	1.01	1.10	1.17	0.77	0.91	1.03
6	3.92	0.97	0.75	0.81	0.87	0.57	0.70	0.78
7	2.18	1.20	0.92	1.00	1.08	0.70	0.84	0.96
8	2.64	1.24	0.96	1.03	1.11	0.74	0.87	0.99
9	3.08	1.42	1.09	1.19	1.07	0.84	1.00	1.14
10	3.16	1.26	0.99	1.05	1.12	0.75	0.88	1.01
11	6.84	1.23	0.95	1.03	1.10	0.73	0.86	0.99
12	3.06	1.01	0.78	0.85	0.90	0.60	0.71	0.81
13	3.27	0.98	0.75	0.82	0.88	0.58	0.69	0.79
14	4.23	0.92	0.71	0.77	0.82	0.54	0.64	0.74
15	2.66	0.95	1.02	1.11	1.18	0.78	0.93	1.06
16	6.60	1.02	0.79	0.86	0.92	0.62	0.73	0.83
17	3.98	1.10	0.86	0.93	0.99	0.67	0.78	0.89
18	4.70	1.10	0.86	0.93	0.99	0.67	0.78	0.89

TABLE IV (CONTINUED)

RUN NO.	RAINFALL INTENSITY (In/Hr)	RATIO OF AVE. DIAM.	RELATIVE EROSIVITY RATIO OF MOMENTUM			RELATIVE EROSIVITY RATIO OF K.E.		
			V_8/V_N	V_{10}/V_N	V_{12}/V_N	V_8/V_N	V_{10}/V_N	V_{12}/V_N
19	2.08	1.26	0.97	1.06	1.13	0.75	0.89	1.01
20	3.52	0.95	0.73	0.80	0.85	0.57	0.67	0.76
21	4.87	0.77	0.59	0.65	0.69	0.46	0.54	0.62
22	4.84	0.90	0.69	0.75	0.81	0.54	0.63	0.72
23	5.85	1.05	0.77	0.84	0.89	0.56	0.67	0.76
24	2.87	1.24	1.04	1.10	1.14	0.89	0.97	1.05
25	4.67	1.24	0.94	1.02	1.08	0.72	0.84	0.94
26	5.16	1.00	0.79	0.86	0.91	0.63	0.74	0.84
27	2.58	1.48	1.09	1.19	1.27	0.81	0.96	1.09
28	9.89	0.88	0.79	0.82	0.85	0.71	0.77	0.82
29	6.76	0.87	0.77	0.80	0.82	0.68	0.73	0.78
30	3.79	0.92	0.86	0.88	0.90	0.81	0.85	0.89
31	6.76	0.70	0.53	0.55	0.57	0.50	0.54	0.56
32	7.38	0.77	0.70	0.72	0.74	0.63	0.68	0.71
33	6.57	0.77	0.71	0.73	0.75	0.66	0.70	0.74
34	4.97	0.95	0.87	0.90	0.93	0.81	0.86	0.93
35	6.20	0.88	0.59	0.60	0.62	0.57	0.60	0.63
			$A_v = 0.864$	$A_v = 0.946$	$A_v = 1.02$	$A_v = 0.706$	$A_v = 0.813$	$A_v = 0.910$

- 55 -

CHAPTER V

SUMMARY AND CONCLUSIONS

A laboratory simulated rainfall is an important research tool for erosion studies. It is generally more rapid, efficient, controlled and adaptable than natural rainfall. However, to simulate rainfall is a very difficult task especially when simulation of both the drop terminal velocity and size distribution are required as in the case for erosion study. A nozzle simulator provides good simulation of the former, but fails to the latter, while a drip simulator usually gives better control on drop size but short on velocity simulation.

In this study, a new type of rainfall simulator was developed which utilized dynamic pressure pulses to eject water drops at an initial velocity such that terminal velocity of the water drop may be attained within a much shorter distance of fall. The drop size is controlled by the magnitude of the pressure pulses and the duration of each pulse application (valve rotation speed). The simulated rainfall intensity is measured as the result of the drop size and ejection frequency. These are controlled by motor speed and number of trippings during each revolution.

As a result of tests run, the following conclusions can be drawn for this newly developed rainfall simulator:

1. A potential for natural rainfall simulation is possible by using pressure pulse water drop ejection method.

2. Some scatter of the data is believed to be a result of imprecision in operating pressure control and measurement.

3. Computed results based on project velocities show that for a given drop diameter, the indexes of momentum and kinetic energy are well simulated at a medium operating pressure range (10 to 15 psi, or 6.895 to 10.34 N/cm²) and allow a 10 to 12 feet (3.05 to 3.66 m) of fall.

4. Simulation of low intensity rainfall was achieved by applying low operating pressure. However, the average drop diameter of the simulated rainfall was larger than that of natural rainfall of the same intensity. On the other hand, if very high operating pressure is used to produce high rainfall intensity, the mean drop diameter of the simulated rain is generally smaller than that of natural rain. These may be described as the characteristics of the simulator. To improve the former, a different ejection hole size may be required to reduce the lower size limit of drops at low pressure magnitude. For high rainfall intensity, medium operating pressure combined with high drop frequency is recommended since extremely

large water drops with corresponding high velocity which are ejected by high pressure tends to break into smaller drops under the resistance of air. This is due to the fact that large water drops are much easier to be distorted to oblate shape and eventually breaks to smaller drops.

5. Some improvements can be made in the future design of the same type simulator in order to make better calculated rainfall control. These include using more precise pressure control (pulse supply and release) devices and better water supply control mechanism for more uniform water distribution to individual modules.

6. As a soil erosion research tool, this unique simulator provides good relative erosivity ratio.

REFERENCES

1. Ellison, W. D. and Pomerene, W. H., "A Rainfall Applicator" Agriculture Engineering, Vol. 25, No. (6), 1944, p. 220.
2. Parsons, Donald A., Discussion of "The Application and Measurement of Artificial Rainfall on Types FA and F in filtrometer". Amer. Geophys. Union Trans. 24; 455-487, 1943.
3. Ekern, P. C., Jr., and Muckenhirn, R. J. "Waterdrop Impact as a Force in Transporting Sand". Soil Sci. Soc. Amer. 12; 441-444, 1947.
4. Mutcher, C. K. and Moldenhauer, W. C., "Applicator for Laboratory Rainfall Simulator", Transactions A.S.A.E., Vol. 5-7, 1963, pp. 220-222.
5. Palmer, Robert S., "An Apparatus for Forming Water-drop", Production Research Report No. 63, U.S. Department of Agriculture, 1962.
6. Grace, Robert A. and Eagleson, Peter S., "Scale Model of Urban Runoff From Storm Rainfall", Journal of the Hydraulics Division, A.S.C.E., Volume 93, No. HY3, May 1967, pp. 161-164.
7. Laws, Otis J., "Measurements of the Fall-Velocity of Water-Props and Raindrops", Transactions, American Geophysical Union, Vol. 22, 1941, pp. 709-721.
8. Lowdermilk, W. C. "Influence of Forest Litter on Runoff Percolation and Erosion" Journal Forestry 28, 474-491, 1920.
9. Craddock, G. W. and Pearse, C. K., "Surface Runoff and Erosion on Granitic Mountain Soil of Idaho as Influences by Range Cover, Soil Distrubance, Slope and Precipitation Intensity", USDA Cir. 482, 1938.
10. Duley, F. L. and Hays, O. E., "The Effect of the Degree of Slope on Runoff and Soil Erosion," Journal Agr. Research 45; 349=360, 1932.
11. Nichols, M. L. and Sexton, H. D. "A Method of Studying Soil Erosion", Agr. Engr. 13: (4) 101-103, 1932.

12. Wilm, H. G., "The Application and Measurement of Artificial Rainfall on Type FA and F Infiltrimeters", Trans. Am Geophys. Un. 24: 480-487, 1943.
13. Meyer, L. D. and McCune, D. L., "Rainfall Simulator for Runoff Plots", Agr. Engr. 39; 644-64, 1958.
14. Hermsmeier, L. F., Meyer, L. D., Barnett, A. P., and Young, R. A., "Construction and Operation of a 16-Unit Rainulator", ARS 41-62, Agr. Res. Service, USDA, March 1963.
15. Bubenzer, G. D. and Meyer, L. D., "Simulation of Rainfall and Soils for Laboratory Research", Transactions of the ASAE, Vol. 8, No. 1, pp. 73-75, 1965.
16. Swanson, N. P., "Rotating Boom Rainfall Simulator", Trans. ASAE, 8; 71-72, 1965.
17. Shachori, A. and Segimer, I. "Sprinkler Assembly for Simulation of Design Storms as a Means for Erosion and Runogg Studies". Bull. Int. Assn. Sci. Hydrol. 7: (4) 57-71, 1962.
18. Gunn, Ross and Kinzer, Gilbert D., "The Terminal Velocity of Fall for Water Droplets in Stagnant Air", Journal of Meterology, 6, 1949, 243-248.
19. Morin, J., Goldberg, D. and Seginer, Ido, "A Rainfall Simulator with a Rotating Disk", Trans. ASAE 74-79, 1967.
20. Laws, J. O and Parsons, D. A., "Relation of Raindrop-soze to Intensity", Trans. Am. Geophys, Un. 24: 452-460, 1943.
21. Meyer, L. D., "Simulation of Rainfall for Soil Erosion Research", Trans. ASAE, 8:1, 63-65, 1965.

NOTATION

C_d	-	coefficient of drag
d	-	rain drop diameter, L
D	-	rain drop stain diameter, L
D_N	-	natural rain drop diameter, L
D_S	-	simulated rain drop diameter, L
e	-	exponential
F_d	-	drag force due to air resistance, F
F_w	-	gravitational force acting on the water drop, F
g	-	gravitational acceleration, L/T^2
m	-	mass of the water drop, M
r	-	constant term
Re	-	Reynolds Number
S	-	distance of fall, L
Δs	-	incremental distance, L
t	-	time in seconds, T
V_N	-	terminal velocity of natural raindrop, L/T
V_O	-	initial velocity, L/T
V_S	-	velocity of simulated raindrop, L/T
ρ_a	-	density of air, M/L^3
ρ_w	-	density of water, M/L^3
Λ	-	constant term
Φ	-	constant term